

ISSN: 3081-1562

Indexed in: Embase/Excerpta Medica,
EBSCOhost, Scopus, SJCR, CINAHL, SciELO,
Latindex, Biblat, CONAHCYT

Archivos de Neurociencias

Volume 30. Number 4, October-December 2025

www.archivosdeneurociencias.mx



SALUD
SECRETARÍA DE SALUD



INSTITUTO NACIONAL
DE NEUROLOGÍA Y
NEUROCIROLOGÍA



PERMANYER
www.permanyer.com

Original papers should be deposited in their electronic version through the following URL:

<https://archivosdeneurociencias.permanyer.com>



Permalyer
Mallorca, 310 – Barcelona (Cataluña), España
permalyer@permalyer.com

Permalyer México
Temistocles, 315
Col. Polanco, Del. Miguel Hidalgo
11560 Ciudad de México
mexico@permalyer.com



www.permalyer.com

ISSN: 3081-1562

Ref.: 10996AMEX254

Reproductions for commercial purposes:

Without the prior written consent of the publisher, no part of this publication may be reproduced, stored in a retrievable medium or transmitted, in any form or by any means, electronic, mechanical, photocopying, recording or otherwise, for commercial purposes.

Archivos de Neurociencias is an open access publication with the Creative Commons license
CC BY-NC-ND (<http://creativecommons.org/licenses/by-nc-nd/4.0/>).

The opinions, findings, and conclusions are those of the authors. The editors and publisher are not responsible and shall not be liable for the contents published in the journal.

© 2025 Instituto Nacional de Neurología y Neurocirugía. Published by Permalyer.

Archivos de Neurociencias

www.archivosdeneurociencias.mx

Volume 30 - Number 4

Contents

EDITORIAL

- New frontiers in neurosurgery: contributions from the UANL International Congress 2025** 155
José L. Andrade-Valencia and Isaac J. Palacios-Ortiz

CONGRESS ABSTRACTS

157

ORIGINAL ARTICLES

- Brain volumes, cognitive dysfunction, and socioeconomic status in adults with and without Alzheimer's disease: an exploratory data análisis** 163
Alberto Guevara-Tirado

- Possible involvement of dorsal hippocampal G-protein coupled receptor 55 (GPR55) in nicotine-induced conditioned place preference in rats** 172
Oliver A. Colis-Arenas, Angélica Muñoz-Pelayo, Carlos H. López-Lariz, Jesús Chávez-Reyes, and Bruno A. Marichal Cancino

CASE REPORTS

- Idiopathic hypertrophic spinal pachymeningitis: a diagnostic challenge. Case report** 180
César A. Almendárez-Sánchez, Carlos Morales-Valencia, Leonardo Álvarez-Vázquez, Arturo de J. Gómez-Cano, and Antonio Sosa-Nájera
- Removal of non-tumorous ovaries in anti-NMDAR receptor encephalitis. Report of 2 cases and literature review** 184
Ana L. Calderón-Garcidueñas and Diego I. Talavera-Bazán

New frontiers in neurosurgery: contributions from the UANL International Congress 2025

Nuevas fronteras en neurocirugía: contribuciones del Congreso Internacional UANL 2025

José L. Andrade-Valencia*^{ORCID} and Isaac J. Palacios-Ortiz^{ORCID}

Department of Neurosurgery, Universidad Autónoma de Nuevo León, Hospital Universitario Dr. José Eleuterio González, Monterrey, N.L., Mexico

The recent II International Congress of Neurosurgery “In Search of New Frontiers” (March 13-15, 2025, Universidad Autónoma de Nuevo León, Mexico) constituted a setting of high academic and scientific value, bringing together researchers, neurosurgeons, health professionals, and students committed to the advancement of the neurosciences. The call for free papers received 40 submissions, of which the scientific committee selected 15 for inclusion in this issue of *Archivos de Neurociencias* as part of a bilateral commitment to promote transnational research among different centers with neurosurgical training. The Congress served as a fertile platform to showcase innovative projects, clinical experiences, and emerging lines of research that reflect the diversity and strength of our medical and neurosurgical community across various training sites.

In this issue of the journal, readers will find contributions covering diverse aspects of contemporary neuroscience. Particularly noteworthy are advances in technology applied to neurosurgery, with reports on the design and local manufacture of 3D-printed surgical retractors and ports, as well as anatomical models for simulation. These initiatives strengthen surgical training, optimize preoperative planning, and promote accessible solutions in resource-limited settings.

Neurointerventionism also occupies a relevant place in the training and care of patients with central nervous system diseases. Several studies document the use of

optical coherence tomography to assess neoendothelialization following the implantation of flow diverters in cerebral aneurysms, providing promising evidence to refine clinical outcomes and to better understand the biological processes of vascular repair.

Additionally, clinical experiences in complex diseases are included: the surgical approach to neurocysticercosis of the pineal region and the use of bilateral decompressive craniectomy in severe traumatic brain injury illustrate the technical adaptability and clinical judgment of our teams when facing scenarios of high morbidity and mortality, contributing practical examples for decision-making in critical settings.

Interest in emerging therapies is reflected in contributions exploring deep brain stimulation as a strategy for motor recovery in spinal cord injury, and radiomodulation for epilepsy secondary to arteriovenous malformations. These lines of work open a therapeutic horizon and lay the groundwork for future clinical trials.

In the field of prognosis, 2 quantitative approaches stand out: the analysis of optic nerve sheath diameter by computed tomography as a possible mortality factor in patients with traumatic brain injury, and a predictive model for postoperative epileptic seizures in intra-axial tumors. Both studies underscore the need for objective and reproducible tools for a truly ethical medicine based on scientific evidence.

Beyond the results, it is worth emphasizing the philosophy that guided this activity: critical peer exchange,

*Correspondence:

José L. Andrade-Valencia
E-mail: joseandvall@gmail.com

Date of reception: 03-11-2025
Date of acceptance: 29-11-2025
DOI: 10.24875/ANCE.M25000067

Available online: 18-02-2026
Arch Neurocién (Eng). 2025;30(4):155-156
www.archivosdeneurociencias.mx

methodological rigor, and ethical commitment to the patient. The dynamic of free papers not only disseminates findings but also cultivates a professional attitude open to continuous learning, interdisciplinary collaboration, and excellence.

Each of the works gathered here bears witness to the effort of our community to expand knowledge, improve clinical practice, and explore new therapeutic frontiers. By offering this space, *Archivos de Neurociencias* strengthens academic exchange and

consolidates a culture of collaboration and scientific impact.

We deeply thank the journal's editorial committee for its support of this initiative, the authors for their dedication and commitment to the neurosciences, and Dr. Ángel Martínez Ponce de León for his leadership in organizing the event.

We are convinced that this issue will be of great interest to our readers and a significant contribution to the neuroscientific community.

Neurosurgical tubular retractor: a technological development and commercial feasibility study of a medical device

Gerardo A. De La Rosa-Hernández^{1*}, Zaira Olivares-Rosales¹, José A. Torres-Torres¹, José N. Barragán-Codina², Óscar E. Cervantes-García³, Jorge A. Cantú-Hernández¹, Eduardo Trejo-Olguín¹, Jesús A. Morales-Gómez¹, and Ángel R. Martínez-Ponce de León¹

¹Department of Neurosurgery and Neurological Endovascular Therapy, University Hospital Dr. José Eleuterio González; ²Department of Biomedical Engineering, University Hospital Dr. José Eleuterio González; ³Department of Marketing Strategies and Business Models, School of Accounting and Administration, Universidad Autónoma de Nuevo León, Monterrey, Nuevo León, Mexico

*Correspondence: Gerardo A. De La Rosa-Hernández, E-mail: gerardo.delarosah@uanl.edu.mx

Background: Intracerebral hemorrhage is an acute, rapidly progressive condition with poor prognosis regarding functional outcome and survival. Minimally invasive surgical drainage is currently the treatment of choice.

Objective: To present a locally designed and manufactured minimally invasive access device (NeuroPort, a surgical port) and compare it with similar commercial devices in terms of cost-effectiveness and surgical performance.

Methods: NeuroPort manufacturing consisted of three phases: (1) 3D design of components (obturator, working channel, illumination frame); (2) stereolithography 3D printing using biocompatible resin; and (3) curing, assembly, and sterilization. A comparative analysis was conducted between NeuroPort and commercial surgical ports (BrainPath[®] and ViewSite[®]) evaluating cost, functionality, and accessibility for public and private hospitals. The study was approved by institutional ethics and research committees, and informed consent was obtained from all patients.

Results: We report the case of a 45-year-old man with intracerebral hematoma treated using NeuroPort. Surgery was completed without complications, and follow-up demonstrated significant clinical and functional improvement.

Discussion: NeuroPort demonstrated a major competitive advantage by reducing production costs by up to 96% compared with commercial devices.

Conclusions: NeuroPort is a safe, easy-to-use device that enables minimally invasive management of intracerebral hemorrhage. Given that more than 80% of medical devices in Mexico are imported, NeuroPort represents a high-potential domestic solution, offering advanced treatment at an affordable cost for nearly all socioeconomic groups.

Funding: Department of Neurosurgery and Neurological Endovascular Therapy, Hospital Universitario Dr. José Eleuterio González, Universidad Autónoma de Nuevo León.

Conflicts of interest: The authors declare no conflicts of interest regarding this manuscript.

Right posterior communicating artery aneurysm: case report

Estefany Mendoza-Verdín^{1*}, Santiago González-Alatorre, and Óscar Ramírez-Gómez

Hospital Civil de Guadalajara Fray Antonio Alcalde, Guadalajara, Jalisco, Mexico

*Correspondence: Estefany Mendoza-Verdín, E-mail: estefany.mendozaverdin@gmail.com

Background: Posterior communicating artery aneurysms account for approximately 25% of intracranial aneurysms and commonly arise at the junction of the internal carotid artery and the posterior communicating artery. They frequently cause significant neurological symptoms, especially when compressing adjacent structures or rupturing.

Case presentation: A 19-year-old man presented with progressive oculomotor neuropathy, left hemibody weakness, balance disturbance, and recurrent falls. Neurological examination revealed involvement of cranial nerves III, IV, and VI on the right side, with ptosis, ophthalmoparesis, and reduced photomotor and accommodation reflexes. Imaging confirmed a right posterior communicating artery aneurysm. Comprehensive diagnostic and therapeutic management was implemented to prevent complications and preserve neurological function.

Discussion: Intracranial aneurysms are most commonly located at arterial bifurcations, with a particularly high incidence at the posterior communicating artery. These aneurysms account for approximately 25% of all intracranial aneurysms and 50% of

internal carotid artery aneurysms. Their management requires a carefully planned strategy to ensure complete obliteration while minimizing the risk of ischemia. Surgical success depends on detailed anatomical knowledge, meticulous preoperative planning, and appropriate selection of the optimal surgical approach.

Conclusions: Optimal treatment depends on appropriate patient selection, accurate anatomical understanding, and careful assessment of associated risks.

Funding: This study received no external funding.

Conflicts of interest: This work was conducted independently and without external influence. The authors declare that there are no financial, personal, or professional conflicts of interest.

Neurocysticercosis of the pineal region: neurosurgical management

José C. Rocha-Villegas^{1*}, Christian Rodríguez-Negrete¹, and Alejandro Monroy-Sosa¹

Department of Neurosurgery, Hospital General ISSSTE Tláhuac, Mexico City, Mexico

*Correspondence: José C. Rocha-Villegas, E-mail: drcarlos1606@gmail.com

Background: Neurocysticercosis is now relatively uncommon. Pineal region involvement is rare, and no consensus exists regarding its management.

Objective: To describe the microsurgical anatomy of the pineal region, present surgical management, and report an additional case.

Methods: The microsurgical anatomy of the pineal region was studied, and the surgical approach used in a case of neurocysticercosis of the pineal region is described.

Results: The pineal region has traditionally been considered surgically inaccessible because of the presence of multiple critical vascular structures that represent major obstacles. Nevertheless, surgical access is sometimes required, underscoring the importance of thorough anatomical understanding. We present the case of a 48-year-old woman diagnosed with a cystic lesion of the pineal region and acute obstructive hydrocephalus. The acute condition was initially managed with a third ventriculostomy, followed by a supracerebellar infratentorial microsurgical approach in the sitting position, assisted by endoscopy, achieving a satisfactory outcome.

Discussion: When indicated, endoscopic management of neurocysticercosis is widely recommended for the treatment of hydrocephalus and lesion resection. However, to our knowledge, reported cases involving the pineal region are few, and optimal management remains controversial. Our case demonstrates that microsurgical management of the pineal region is feasible and can complement endoscopic techniques to achieve favorable results.

Conclusions: Although the limited number of reported cases of pineal region neurocysticercosis and the complex microsurgical access to this area may suggest that surgical management is challenging, it is feasible with an adequate understanding of regional anatomy and an integrated surgical approach that combines endoscopic and microsurgical techniques.

Funding: None declared.

Conflicts of interest: None declared.

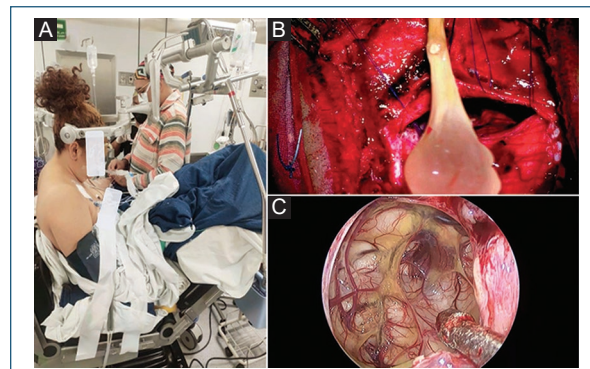


Figure 1. **A:** semi-sitting position for suboccipital craniotomy. **B:** cyst excision. **C:** pineal region confirmed via the supracerebellar infratentorial corridor with arachnoiditis due to neurocysticercosis.

Date of reception: 27-12-2024

Date of acceptance: 26-02-2025

DOI: 10.24875/ANCE.M2500068

Available online: 18-02-2026

Arch Neurocién (Eng). 2025;30(4):157-162

www.archivosdeneurociencias.mx

Exploring potentials: deep brain stimulation for motor recovery after spinal cord injury

Guri Y. Romero-Zuluaga¹, Luis C. Hernández-Jarquín¹, Ingrid M. Reza-Ocampo Marlin¹, Gustavo E. Sánchez-Estrada¹, Dulce P. Estrada-Schott², Luis A. Solís-Zavala¹, and José A. J. Prestegui-Muñoz^{1,3*}

¹National School of Medicine and Homeopathy, IPN; ²Higher School of Medicine, IPN; ³Department of Neurology and Psychiatry, Instituto Nacional de Ciencias Médicas y Nutrición Salvador Zubirán, Mexico City, Mexico

*Correspondence: José A. J. Prestegui-Muñoz, E-mail: j.angel.prestegui@gmail.com

Background: Spinal cord injuries are among the most significant neurosurgical pathologies today, as they damage critical neuroanatomical structures involved in both afferent and efferent signaling. Recently, stimulation of residual lumbar projections through deep brain stimulation (DBS) has been explored as a potentially promising technique for patients with spinal cord injury.

Objective: To analyze the potential use of DBS in patients with disabling spinal cord injuries and to evaluate its impact on quality of life.

Methods: We conducted a literature review using PubMed, the Cochrane Library, and Scopus. The search focused initially on rehabilitation in patients with spinal cord injuries and subsequently on the application of deep brain stimulation in this specific patient population. Inclusion criteria were restricted to studies reporting the use of this therapy.

Results: DBS emerged as an innovative option with a positive impact not only on functional improvement but also on pain management. The studies reviewed demonstrated partial recovery of proximal muscle strength, with a greater effect in the lower extremities, leading to improved ambulation – particularly the ability to ascend and descend stairs without assistance – as well as enhanced voluntary motor control and balance.

Conclusions: Although current evidence regarding the use of DBS for this condition remains limited, existing studies indicate meaningful benefits in locomotor recovery, motor control, and overall patient improvement. These findings highlight a critical direction for future neurosurgical research, underscoring the need for controlled studies to determine long-term efficacy. This therapeutic approach may ultimately serve as an option for patients who have exhausted conventional treatments, provided that strict inclusion criteria are applied.

Funding: The authors declare that no funds, grants, or other forms of support were received during the preparation of this manuscript.

Conflicts of interest: The authors declare no known financial conflicts of interest or personal relationships that could have influenced the work reported in this article.

Surgical management criteria for bilateral lumbar pars fracture in a young athlete: case report

Sergio Díaz-Bello^{1*}, Edith M. Herrera-Mejía², Carlos Morales-Casillas², Guri Y. Romero-Zuluaga², and Xareni B. Falcón-Sánchez²

¹Hospital Ángeles Pedregal; ²National School of Medicine and Homeopathy; IPN. Mexico City, Mexico

*Correspondence: Sergio Díaz-Bello, E-mail: sergio.neurocirugia02@gmail.com

Background: Lumbar spondylolysis is a fatigue fracture of the pars interarticularis of the lumbar lamina that commonly occurs in young athletes and adolescents. Management typically begins with conservative treatment; however, in selected cases, we believe that surgical treatment may represent a viable first-line option.

Objective: To propose an initial surgical strategy in a young professional athlete with bilateral pars fracture, achieving satisfactory outcomes and an earlier return to professional sports activity than would be expected with conservative management alone.

Case presentation: An 18-year-old male professional soccer player with no prior comorbidities presented with mechanical low back pain of 8 months' duration. He underwent 6 months of conservative treatment (rest, nonsteroidal anti-inflammatory drugs, physiotherapy, etc.). Physical examination revealed loss of lumbar lordosis, localized tenderness over and adjacent to the L1–L3 spinous processes, and pain with both passive and active trunk hyperextension. No neurological deficits were observed. Imaging confirmed bilateral pars fractures. The patient underwent bilateral direct isthmic repair at L2. A 6.0 mm x 45-mm titanium screw was placed along the fracture line of the pars toward the pedicle and vertebral body. Postoperatively, the patient maintained a pain score of 3/10 on the Visual Analog Scale, minimal disability on the Oswestry Disability Index, and a score below 4 points on the Roland–Morris Disability Questionnaire.

Discussion: While conservative management remains the cornerstone of treatment, no control group exists to adequately compare the effectiveness of treatment algorithms against surgical management.

Conclusions: In carefully selected patients such as this case, initial surgical treatment may be considered, taking into consideration clinical, radiographic, and occupational characteristics.

Funding: None declared.

Conflicts of interest: The authors declared no conflicts of interest.

Role of radiomodulation in epilepsy due to cerebral arteriovenous malformations: case series

Maximiliano Preciado-Díaz^{1,2*}, Everardo García-Estrada¹, Jorge A. Cantú-Hernández^{1,2}, César B. Cantú-Espinoza^{1,2}, Leopoldo Pérez-García¹, Paula F. Zárate-Hernández^{1,2}, José L. Andrade-Valencia¹, Jesús A. Morales-Gómez¹, and Ángel R. Martínez-Ponce de León¹

¹Department of Neurosurgery; ²Student Chapter of the American Association of Neurological Surgeons, Hospital Universitario Dr. José Eleuterio González, Universidad Autónoma de Nuevo León, Monterrey, Mexico

*Correspondence: Maximiliano Preciado-Díaz, E-mail: maxmtydiaz@hotmail.com

Background: Epilepsy is a frequent clinical manifestation in patients with cerebral arteriovenous malformations (AVMs) and significantly affects quality of life. Stereotactic radiosurgery (SRS) has become a relevant therapeutic option because of its precision and limited impact on healthy tissue; however, its effectiveness in AVMs located within eloquent brain regions remains challenging.

Objective: To evaluate the effect of SRS and radiomodulation on reducing seizure frequency in patients with epilepsy secondary to AVMs.

Methods: Seven patients with unruptured AVMs were treated with SRS using the CyberKnife system at doses below 30 Gy and followed clinically for 12 months. Variables analyzed included seizure control and functional outcomes. Mean nidus size was 24.87 ± 15.65 mm, with 2.71 ± 1.69 afferent feeders. According to the Spetzler–Martin classification, 28.57% were grade II, 42.86% grade III, and 28.57% grade IV. AVMs were located in frontotemporal (n = 2), occipital (n = 2), frontoparietal (n = 1), temporal (n = 1), and parieto-occipital (n = 1) regions. Four patients received single-session SRS (21 ± 5.39 Gy), and three received fractionated SRS (26.67 ± 2.39 Gy); three patients also underwent embolization (Table 1).

Table 1. Arteriovenous morphology characteristics and treatment

Case No.	Sex	Age (y)	Location	Size (mm)	No. of feeders	Eloquent area
1	M	17	Frontotemporal (right)	1.75	4 (1.84)	+
2	M	10	Frontotemporal (left)	6.23	1 (0.58)	+
3	F	18	Occipital (right)	24.7	2 (1.11)	+
4	F	37	Frontoparietal (right)	30.4	4 (2.69)	+
5	M	17	Temporal (right)	35.2	3 (2.00)	+
6	M	7	Occipital (left)	24.8	1 (0.58)	–
7	M	21	Parieto-occipital (left)	51.3	4 (2.31)	+

Case No.	S–M Grade	Ruptured	mRS Outcome	Embolization	Radiosurgical treatment	
					Radiosurgery type	Total dose (Gy)
1	III	+	Poor	–	Single session	20
2	II	+	Poor	–	Single session	16
3	III	–	Good	+	Single session	16
4	II	–	Good	+	Fractionated	25
5	IV	–	Good	+	Fractionated	30
6	III	+	Poor	–	Single session	18
7	IV	–	Good	+	Fractionated	25

mRS: modified Rankin Scale; S–M; Spetzler–Martin.

Results: All patients experienced a significant reduction in ictal activity, achieving 100% seizure control. The best functional outcomes were observed in patients who received embolization combined with single-session SRS.







Discussion: Radiomodulation using subablative or hypofractionated regimens may reduce cortical excitability, contributing to seizure control even without complete AVM obliteration. These findings suggest a beneficial effect beyond simple anatomical elimination of the lesion.

Conclusions: SRS represents a promising noninvasive therapeutic alternative for controlling epilepsy secondary to AVMs, particularly in eloquent brain regions. Additional studies are required to optimize treatment protocols and validate the durability of the observed clinical effect.

Funding: This study was supported institutionally by Universidad Autónoma de Nuevo León through the Department of Neurosurgery and Neurological Endovascular Therapy at Hospital Universitario Dr. José Eleuterio González. No external funding was received.

Conflicts of interest: The authors declare no conflicts of interest.

3D model for surgical technique planning and practice: development

Jan P. Camarillo-Ortiz¹, Karolina Mendoza-Garza¹, Kristen M. Salais-Torres¹, Gerardo A. De La Rosa-Hernández¹, Oscar E. Cervantes-García², Jorge A. Cantú-Hernández¹, Jesús A. Morales-Gómez¹, and Ángel R. Martínez-Ponce de León¹

¹Neurosurgery and Neurological Endovascular Therapy Service; ²Department of Biomedical Engineering. Hospital Universitario Dr. José Eleuterio González, Universidad Autónoma de Nuevo León, Monterrey, Nuevo León, Mexico

*Correspondence: Jan P. Camarillo-Ortiz, E-mail: jan.camarilloor@uanl.edu.mx

Background: This project consists of the development of a scaled 3D-printed model of the cranial vault, designed for practicing the surgical technique of trephination, a procedure involving the creation of one or more circular openings through the thickness of the cranial vault walls.

Objective: The main objective is to provide physicians in specialist training with a practical and realistic simulation tool.

Methods: We conducted a descriptive technical study for the creation of 3D cranial vaults for neurosurgical training purposes. Using DICOM files from computed tomography scans, digital models were generated in 3D Slicer and InVesalius. STL files were edited in Meshmixer to repair and adapt osseous structures. They were subsequently prepared in PreForm (Formlabs), where supports and materials were defined. Printing was performed using stereolithography with photosensitive Clear Resin V4.0, with an approximate duration of 7 h 20 min per model. After printing, the models were washed in isopropyl alcohol to remove residues and UV-cured to obtain final strength. The complete printing and post-processing process took approximately 9 h. The models were used in burr-hole craniotomy simulations to evaluate their usefulness in surgical planning and specialized medical training.

Results: An example of model use is presented, in this case oriented toward approaches to the lateral aspect of the cranial vault. Anatomical identification of surgical sites for burr-hole placement was performed, as well as hands-on management of the surgical instruments required for the procedure.





Discussion: Participants in the training exercise, who already had surgical experience, reported feeling comfortable with the model.

Conclusions: This is a practical, low-cost model with a high level of anatomical detail that enables simulation of neurosurgical approaches. Although the initial results are promising, additional studies are required to evaluate the long-term impact of this tool on medical education and the performance of neurosurgical trainees, with potential to optimize training and preoperative planning in neurosurgery.

Funding: Servicio de Neurocirugía y Terapia Endovascular Neurológica, Hospital Universitario Dr. José Eleuterio González, Universidad Autónoma de Nuevo León.

Conflicts of interest: The authors declare that there are no conflicts of interest regarding the publication of this manuscript.

Neoendothelialization process in wide-neck aneurysms after flow diverter implantation: findings using technology

José J. Gutiérrez-Baños^{1,2,3*}, Mauricio I. Rodríguez-Pereira^{1,2}, Jorge O. López-Esparza⁴, Daniel Dávila-Rodríguez¹, Jecsán Tovar-Fuentes^{2,3}, Alondra S. Tovar-Jiménez^{2,3}, Boris L. Pabón-Guerrero⁵, and Juan A. Hernández-López^{2,3}

¹Department of Neurosurgery, Hospital Regional 1.º de Octubre, Instituto de Seguridad y Servicios Sociales de los Trabajadores del Estado, Mexico City, Mexico; ²Neurosurgery Endovascular Therapy, Stroke Team México, Mexico City, Mexico; ³Neurosurgical Research, Universidad Autónoma del Estado de Hidalgo, Pachuca, Hidalgo, Mexico; ⁴Vascular and Endovascular Neurology, Hospital General de León, León, Guanajuato, Mexico; ⁵Department of Endovascular Neurosurgery, Angio Team, Medellín, Antioquia, Colombia

*Correspondence: José J. Gutiérrez-Baños, E-mail: josegutierrezbanosmd@gmail.com

Background: Optical coherence tomography (OCT) has demonstrated utility in evaluating neoendothelialization of wide-neck aneurysms treated with the Flow Redirec-

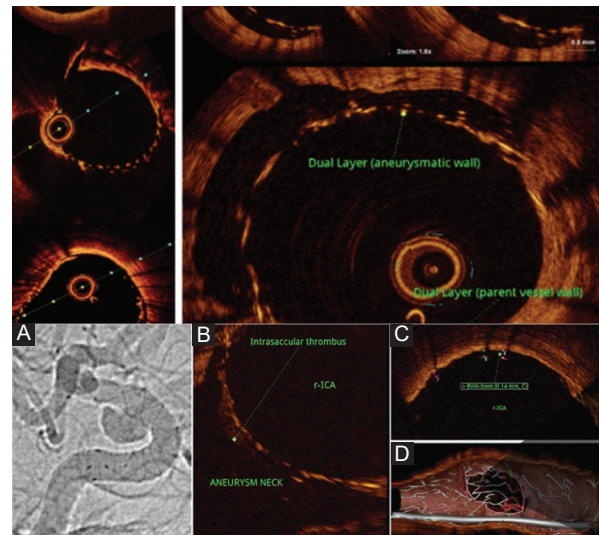


Figure 1. Neoendothelialization process in wide-neck aneurysms.

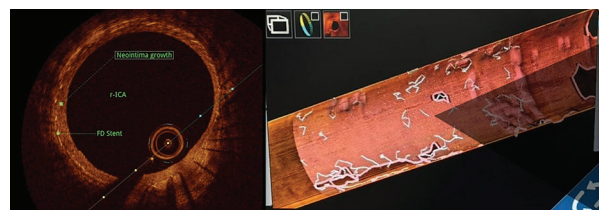


Figure 2. Neoendothelialization.

tion Endoluminal Device (FRED). FRED devices are designed to redirect blood flow in intracranial aneurysms, promoting neoendothelialization and aneurysm occlusion. OCT provides high-resolution intravascular imaging, allowing detailed assessment of neointimal formation and stent apposition – key factors for effective aneurysm healing.

Objective: To evaluate healing of wide-neck aneurysms treated with FRED using OCT; analyze thrombus formation, neoendothelialization, and device apposition; and correlate OCT findings with clinical evolution.

Methods: We conducted a study in a 79-year-old woman diagnosed with an internal carotid artery aneurysm. A FRED was implanted, and postoperative OCT evaluation was performed at a pullback speed of 18 mm/s with 30 mL of contrast medium. The images obtained allowed analysis of neoendothelialization, presence of thrombosis, and patency of adjacent perforating vessels.

Results: A total of 152 high-quality images were analyzed, demonstrating excellent apposition of the FRED to the arterial wall (range 5–22 µm) and progressive neoendothelialization, without evidence of significant thrombosis. No thromboembolic complications were reported during postoperative follow-up.



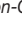

Discussion: OCT outperforms conventional angiography by providing more detailed imaging for assessing FRED integration, thrombosis, and endothelialization. This technology optimizes postoperative management and may predict treatment success. Although its application in tortuous intracranial vessels presents technical challenges, its diagnostic precision is invaluable.

Conclusions: These results suggest that OCT is a promising tool that provides detailed visualization of the healing process after FRED implantation, offering information on neointimal formation and stent apposition – fundamental aspects for successful treatment of wide-neck aneurysms. This technology may help predict outcomes and optimize patient management strategies (Figs. 1 and 2).

Funding: Self-funding and material resources provided by ISSSTE.

Conflicts of interest: The authors declare that the content of this article was prepared without commercial or financial relationships that could be interpreted as a conflict of interest.

OCT Technology in the neuroendovascular field: step-by-step use of the dragonfly OCT catheter

José J. Gutiérrez-Baños^{1,2,3*}, Mauricio I. Rodríguez-Pereira^{1,2}, Jorge O. López-Esparza⁴, Daniel Dávila-Rodríguez¹, Jecsán Tovar-Fuentes^{2,3}, Alondra S. Tovar-Jiménez^{2,3}, Boris L. Pabón-Guerrero⁵, and Juan A. Hernández-López^{2,3}

¹Department of Neurosurgery, Hospital Regional 1.º de Octubre, Instituto de Seguridad y Servicios Sociales de los Trabajadores del Estado, Mexico City, Mexico; ²Neurosurgery

Endovascular Therapy, Stroke Team México, Mexico City, Mexico; ³Neurosurgical Research, Universidad Autónoma del Estado de Hidalgo, Pachuca, Hidalgo, Mexico; ⁴Vascular and Endovascular Neurology, Hospital General de León, León, Guanajuato, Mexico; ⁵Department of Endovascular Neurosurgery, Angio Team, Medellín, Antioquia, Colombia

*Correspondence: José J. Gutiérrez-Baños, E-mail: josegutierrezbanosmd@gmail.com

Background: Optical coherence tomography (OCT) has evolved from its original use in ophthalmology into a valuable tool for the visualization of vascular structures and endovascular devices. Its application in the neurovascular field has been limited by the tortuosity of intracranial vessels, which complicates access with rigid devices.

Objective: To evaluate the usefulness of OCT technology and the Dragonfly OCT catheter for visualizing in-stent thrombus, assessing endovascular device apposition to the vessel wall, and evaluating stent conformability in the neuroendovascular field.

Methods: Randomly selected patients provided informed consent. An 8 Fr introducer sheath, a Neuron Max 0.88 catheter, and a Sofia 6F distal access catheter with a 0.014" microguidewire were used. OCT images were acquired using the Dragonfly Optis Imaging system at a pullback speed of 18 mm/s with injection of 30 mL of contrast medium. Thrombus and device–vessel wall interactions were evaluated.

Results: Images demonstrated in-stent thrombus (white and red) and allowed assessment of apposition of FRED and CASPER devices to the vessel wall. OCT proved reliable for evaluating neointimal quality and vessel patency, outperforming other techniques in the assessment of thrombus and device conformability.

Discussion: The use of OCT in intracranial vessels continues to face challenges due to vascular tortuosity; however, devices such as the Dragonfly OCT catheter have improved navigability. Although additional multicenter studies are required, OCT has demonstrated superiority over other techniques, particularly in the evaluation of thrombus and endovascular device conformability.

Conclusions: OCT is a promising tool for evaluating in-stent thrombus and endovascular device–vessel interactions in the neuroendovascular field. Further studies are required for its validation as a standard evaluation method.

Funding: Self-funded; material resources provided by ISSSTE.

BRAINNN Score: a therapeutic proposal for epileptic seizures in patients operated on for intra-axial tumors

Sergio Díaz-Bello^{1*}, Edith M. Herrera-Mejía², Carlos Morales-Casillas², Guri Y. Romero-Zuluaga², and Xareni B. Falcón-Sánchez²

¹Hospital Ángeles Pedregal; ²Escuela Nacional de Medicina y Homeopatía del IPN, Mexico City, Mexico

*Correspondence: Sergio Díaz-Bello, E-mail: sergio.neurocirugia02@gmail.com

Background: Epileptic seizures (ES) are a frequent primary manifestation of central nervous system tumors and significantly affect patient quality of life. Some patients do not present seizures at diagnosis but may develop seizures or epilepsy following surgical treatment. A thorough understanding of predictive factors for seizure development and postoperative seizure freedom is essential in the management of brain tumors. Therefore, we analyzed risk factors for postoperative seizure development in patients without preoperative seizures.

Objective: To determine risk factors for postoperative epileptic seizures in patients with intra-axial tumors and propose a decision-making scale for therapeutic management.

Methods: We conducted a retrospective, observational study. All patients with histopathological diagnosis of intra-axial tumors (gliomas, metastases, and lymphomas) without preoperative seizures were included. Potential risk factors were recorded, followed by logistic regression analysis to determine significantly associated factors and calculation of odds ratios for postoperative seizure risk.

Results: The Neuro-oncology/Emergency database of the Instituto Nacional de Neurología y Neurocirugía (n = 10,827) was analyzed; 446 patients met inclusion criteria. Of these, 345 had gliomas (48% low-grade and 52% high-grade), 73 had metastases, and 28 had primary lymphomas.

Discussion: A total of 417 patients were eligible for logistic regression, and 5 factors were significantly associated with postoperative seizures: (1) age < 40 years; (2) gliomas; (3) significant edema; (4) incomplete resection; and (5) frontal location. When ≥ 3 criteria were present, more than 92% of patients developed postoperative seizures.

Conclusions: Prophylactic treatment in patients without pre-treatment seizures is not recommended.

Funding: None declared.

Conflict of interest: The authors declare no conflicts of interest.

Bilateral decompressive craniectomy in a teaching hospital: a last resort for the management of severe traumatic brain injury

Eduardo Trejo-Olguín¹, Edgar O. Rodríguez-Guajardo¹, José L. Andrade-Valencia¹, Ángel R. Martínez-Ponce de León¹, and Jesús A. Morales-Gómez¹

Universidad Autónoma de Nuevo León, Monterrey, Nuevo León, Mexico

*Correspondence: Eduardo Trejo-Olguín, E-mail: etrejo1989376@uanl.edu.mx

Objective: We present two cases treated at a university hospital in Mexico using bilateral decompressive craniectomy for the management of patients with severe traumatic brain injury (TBI).

Methods: Case 1: A 34-year-old man presented with severe TBI after blunt head trauma. He exhibited altered level of consciousness, generalized tonic-clonic seizures, a Glasgow Coma Scale (GCS) score of 4, 2-mm pupils, and computed tomography showing subarachnoid hemorrhage and refractory cerebral edema.

Case 2: A 51-year-old man sustained severe TBI after a fall from 3 meters. He presented with altered consciousness, a GCS score of 3, and 3-mm hyporeactive pupils. CT revealed temporal intraparenchymal hematomas measuring 7 cc in the left hemisphere and 5 cc in the right hemisphere.

Results: Both patients underwent bilateral decompressive craniectomy, achieving a postoperative GCS score of 11. They were discharged with tracheostomy and gastrostomy, with a Glasgow Outcome Scale score of 3, and one patient achieved a Karnofsky Performance Score of 90.

Discussion: The prognosis of severe TBI is generally poor. In the present cases, a previously described surgical technique with high morbidity was used as a last-resort treatment and resulted in favorable clinical evolution, improving morbidity and mortality outcomes.

Conclusions: Bilateral decompressive craniectomy may represent a surgical option in selected patients who are refractory to conventional management, particularly in resource-limited settings. Further studies are required to assess its effectiveness and long-term prognosis.

Funding: Institutional resources of the department.

Conflicts of interest: The authors declare no conflicts of interest.

Optic nerve sheath diameter on computed tomography as a prognostic factor in traumatic brain injury

José L. Andrade-Valencia¹, Christian F. Montiel¹, Jorge A. Cantú-Hernández¹, Paula F. Zárate-Ángeles¹, Frida Valle-Domínguez¹, Juan M. Vicencio-Hernández¹, Jesús A. Morales-Gómez¹, and Ángel R. Martínez-Ponce de León¹

Neurosurgery and Neurological Endovascular Therapy Service, Hospital Universitario Dr. José Eleuterio González, Universidad Autónoma de Nuevo León, Monterrey, Nuevo León, Mexico

*Correspondence: José L. Andrade-Valencia, E-mail: joseandvall@gmail.com

Background: Non-contrast head CT is the ideal initial imaging modality for traumatic brain injury (TBI). Previous studies suggest that increased optic nerve sheath diameter (ONSD) is an indirect sign of intracranial hypertension and may serve as a mortality indicator in TBI.

Objective: To evaluate the ability of CT-measured ONSD to predict mortality in patients with TBI.

Methods: We conducted an observational, analytical, retrospective study. Inclusion criteria were age ≥ 18 years, TBI diagnosis, hospitalization within 24 hours of injury, and availability of baseline and postoperative CT scans. ONSD measurements were performed on both scans by a single evaluator.

Results: A total of 68 patients were included; 65 (95.6%) were men. Median age (IQR) was 41 years (31–58). The most common presentation was mild TBI (56.7%), subdural hematoma (41.5%), and Rotterdam score ≥ 3 (54.4%). 42 patients (61.8%) underwent surgical treatment. Mean ONSD was 4.67 ± 0.99 mm. During hospitalization, 7 patients (10.3%) died. In multivariable logistic regression among surgically treated patients, adjusted for admission Rotterdam score and GCS, postoperative reduction of ONSD showed a non-significant protective trend for mortality (aOR 0.33; 95% CI, 0.06–1.73; P = .19).

Conclusions: Reduction of CT-measured ONSD is an accessible parameter that may help predict mortality in surgically treated TBI patients. Larger studies are needed to define its prognostic value and standardize its clinical use.

Funding: Institutional support from Universidad Autónoma de Nuevo León through Hospital Universitario Dr. José Eleuterio González; no external funding.

Conflicts of interest: The authors declared no conflicts of interest whatsoever.

Table 1. Clinical and tomographic characteristics of patients

Variable	Total (n = 68)	Survivors (n = 61)	Deceased (n = 7)	P
Male sex	65 (95.6%)	58 (95.1%)	7 (100%)	0.99
Median age (IQR), y	41 (31–58)	41 (31–58)	41 (30–49)	0.92
Moderate/Severe TBI	29 (43.3%)	24 (40.0%)	5 (71.4%)	0.22
Hematoma location				
Epidural	23 (35.4%)	22 (37.9%)	1 (14.3%)	0.14
Subdural	27 (41.5%)	24 (41.4%)	3 (42.9%)	0.82
Subarachnoid hemorrhage	10 (15.4%)	9 (15.5%)	1 (14.3%)	0.16
Intracerebral hemorrhage	5 (7.7%)	3 (5.2%)	2 (28.6%)	0.53
Dominant hemisphere	34 (53.1%)	31 (53.4%)	3 (42.8%)	0.99
Rotterdam CT score				
1	13 (19.1%)	12 (19.7%)	1 (14.3%)	0.76
2	18 (26.5%)	18 (29.5%)	0 (0%)	
3	17 (25.0%)	16 (26.2%)	1 (14.3%)	
4	12 (17.6%)	7 (11.5%)	1 (14.3%)	
5	8 (11.8%)	8 (13.1%)	5 (71.4%)	
Initial ONSD, mean (SD), mm	4.67 (0.99)	4.69 (0.98)	3.87 (0.57)	-
Surgical treatment	42 (61.8%)	38 (62.3%)	4 (57.1%)	-
Length of stay, median (IQR), d	7 (5–12)	7 (5–12)	7 (3–13)	-

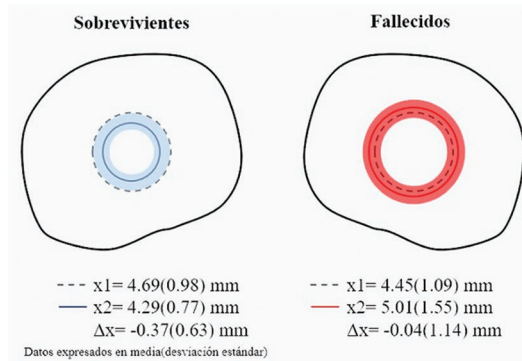


Figure 1. Decrease in optic nerve sheath diameter (ONSD) in surviving and deceased patients.

Pneumorrhachis, pneumocephalus, and intraspinal abscess due to metastatic rectal adenocarcinoma: case report

M. Eugenia Calvillo-Aranda¹, Manuel F. Sánchez-González², Sofía A. Flores-López¹, Jesús A. Morlet-Chávez², and Daniela A. Medina-Rodríguez¹

¹Department of Health Research, Faculty of Medicine, Saltillo Unit, Universidad Autónoma de Coahuila; ²Department of Neurosurgery and Endovascular Therapy, Hospital Christus Muguerza, Saltillo, Coahuila, Mexico

*Correspondence: M. Eugenia Calvillo-Aranda, E-mail: mariaravacal@gmail.com

Background: Pneumorrhachis and pneumocephalus are rare findings, usually associated with trauma, medical procedures, or, rarely, infections. Their occurrence in oncology patients is extremely uncommon.

Objective: To demonstrate the atypical presence of *Escherichia coli* in pneumorrhachis, pneumocephalus, and intraspinal abscess secondary to metastatic rectal adenocarcinoma.

Methods: A 47-year-old woman with stage IV rectal adenocarcinoma was evaluated through full clinical examination, laboratory tests (CBC, procalcitonin, CSF), and abdominal and cranial CT.

Results: The patient presented with severe hypogastric pain (VAS 9/10), induration in the right iliac fossa, muscle hypotrophy, and hyperreflexia. CT demonstrated bowel obstruction and intraspinal abscess. She later developed severe headache (VAS 8/10); cranial CT revealed air in the posterior fossa and suprasellar region. S1 laminectomy revealed purulent drainage. CSF showed neutrophilic pleocytosis, hypoglycorrhachia,

hyperproteinorrhachia, and *E. coli* growth.

Discussion: Combined management (surgical drainage, targeted antibiotics, colostomy) stabilized neurological status, but the patient later died from metastatic progression. This case highlights an exceptional etiology of pneumorrhachis: tumor invasion with necrosis and *E. coli* abscess formation. Dural disruption caused by metastasis, together with chemotherapy-induced immunosuppression, facilitated bacterial migration and gas formation. *Escherichia coli*, identified as the causative pathogen in 14.1% of septic pneumorrhachis cases, accounted for the observed neutrophilic pleocytosis and acute clinical presentation (headache and neuropathic pain), which is unusual in these conditions (only 9% are symptomatic). Computed tomography was crucial for diagnosis and surgical planning.

Conclusions: In cancer patients presenting with acute neurological symptoms and intraspinal gas, although multidisciplinary management and oncologic control may mitigate local complications, infectious and necrotic etiologies must be strongly suspected.

Funding: This project received no funding.

Conflicts of interest: The authors report no conflicts of interest.

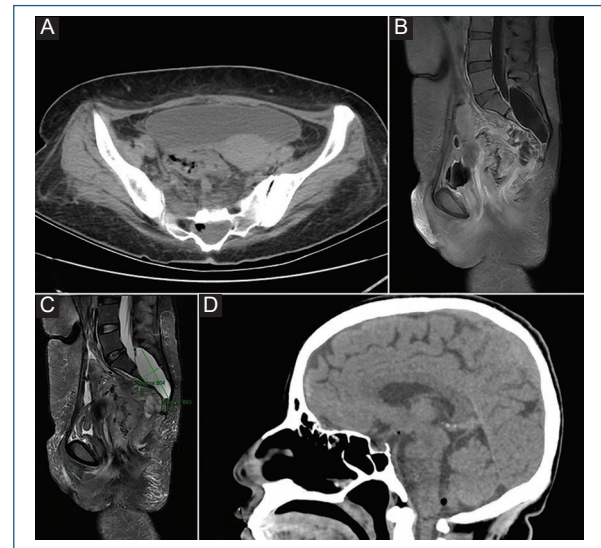


Figure 1. A: non-contrast CT at the sacral level showing disruption of the anterior wall and S5 vertebral body, with a heterogeneous 40-cc collection exerting mass effect on the spinal canal and containing air bubbles. B: contrast-enhanced CT showing collections with peripheral contrast enhancement. C: STIR MRI sequence showing an intraspinal collection with CSF-like characteristics. D: pneumocephalus in the posterior fossa and supratentorial region.

Minimally invasive evacuation of spontaneous intraparenchymal hematoma using a low-cost transcortical port system: case report

Samuel Pérez-Carranza¹, Jesús A. Morales-Gómez², Ángel R. Martínez-Ponce de León², Benny Vázquez-Martínez², and José L. Andrade-Valencia²

Department of Neurosurgery, Hospital Universitario Dr. José Eleuterio González, Monterrey, Nuevo León, Mexico

*Correspondence: Samuel Pérez-Carranza, E-mail: spc.esm@gmail.com

Background: Spontaneous intracerebral hemorrhage accounts for approximately 10–15% of all cerebrovascular events and is associated with high mortality and disability rates. Surgical treatment has evolved toward minimally invasive techniques, such as transcortical port–assisted evacuation, aimed at minimizing tissue injury and improving neurological recovery.

Objective: To present a case of spontaneous intraparenchymal hematoma evacuation using a low-cost surgical port system, highlighting the technique, postoperative outcomes, and clinical course.

Methods: We report the case of a 50-year-old man with a history of hypertension who presented with sudden alteration of consciousness, a Glasgow Coma Scale score of 13, and dense left-sided hemiparesis (2/5 on the Lovett scale). Cranial computed tomography revealed a 64-cc hematoma in the right basal ganglia with 10-mm midline shift from right to left (Fig. 1A). A minimally invasive surgical procedure was performed using a low-cost illuminated port system manufactured by 3D printing at the Department of Neurosurgery of Hospital Universitario Dr. José Eleuterio González. In the operating room, with the patient intubated and sedated, a frontal burr hole was created at the Kocher point, and a 22-mm diameter transcortical port was inserted (Fig. 1B).

The hematoma was subsequently evacuated by aspiration.

Results: Postoperative cranial CT demonstrated complete evacuation of the intraparenchymal hematoma (Fig. 1C). The patient showed good clinical recovery and was discharged 5 days after surgery. At discharge, neurological examination revealed a Glasgow Coma Scale score of 15, reactive and isocoric pupils (3 mm), and full motor strength (5/5 on the Lovett scale) in all extremities.

Conclusions: Port-assisted evacuation proved to be a safe and effective technique for minimizing cerebral trauma. Compared with conventional methods, this approach demonstrated reduced mortality and improved functional recovery, particularly when combined with adjuvant therapies such as postoperative rehabilitation.

Funding: This research received no specific grant from any funding agency in the public, commercial, or not-for-profit sectors.

Conflicts of interest: The authors declare no conflicts of interest regarding the materials or methods used in this study or the findings reported.

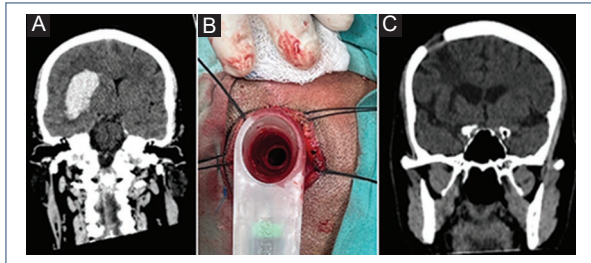


Figure 1. **A:** right intraparenchymal hematoma in the basal ganglia. **B:** transcortical access port. **C:** postoperative CT.

Spontaneous vertebral artery dural arteriovenous fistula without traumatic history: case report

Omar De Paz-Jaimes¹*, Jorge Jacobo-Cruz¹, Juan M. Vicencio-Hernández², Antonio Jiménez-Reyna², José L. Andrade-Valencia¹, Eduardo Trejo-Oguini¹, Jesús A. Morales-Gómez¹, and Ángel R. Martínez-Ponce De León¹

¹Department of Neurosurgery, Hospital Universitario Dr. José Eleuterio González; ²Faculty of Medicine, Universidad Autónoma del Estado de Nuevo León. Monterrey, Nuevo León, Mexico

*Correspondence: Omar De Paz-Jaimes, E-mail: o.depazneuro@gmail.com

Background: Dural arteriovenous fistulas are abnormal connections between arteries and veins within the dura mater; their occurrence in the vertebral artery is extremely rare. Trauma and iatrogenic procedures are recognized predisposing factors.

Objective: To present a clinical case of spontaneous vertebral arteriovenous fistula without evident predisposing factors, highlighting clinical presentation, anatomical location, and treatment.

Case presentation: A 39-year-old man with a past medical history of alcohol use since age 20, active smoking (1725 pack-years), and marijuana use, with no history of trauma, presented with sudden-onset, pulsatile holocranial headache rated 10/10, radiating retro-orbitally to the right, worsened by smoking and without relief. Right hemiparesis and dysarthria subsequently developed. Head CT demonstrated a 1-cc intraparenchymal hematoma in the medulla oblongata with ventricular system disruption. Neurologic exam-

ination revealed a Glasgow Coma Scale score of 14, right hypoglossal nerve palsy, and right hemiparesis graded 3/5 on the Lovett scale, with right-beating horizontal rotational nystagmus, right-sided dysmetria, dysdiadochokinesia, and truncal ataxia. Diagnostic cerebral angiography identified a dural arteriovenous fistula supplied by the right V2 segment with antegrade drainage into the sagittal sinus (Fig. 1A). Selective microcatheterization of the feeding artery was performed, a balloon was positioned in the V2 segment, and balloon-assisted embolization using Onyx was carried out (Fig. 1B and 1C). Follow-up imaging showed complete obliteration of the fistula. Postprocedurally, the patient demonstrated marked clinical improvement with intact cranial nerve function, full motor strength (5/5 on the Lovett scale), normal sensory examination, preserved vestibulo-cerebellar function, and gait with a broadened base of support.

Conclusions: This case is notable for its spontaneous presentation without an identifiable precipitating event. The abrupt onset underscores the importance of including this entity in the differential diagnosis of cerebrovascular disorders to ensure timely and appropriate management.

Funding: This research received no specific grant from any funding agency in the public, commercial, or not-for-profit sectors.

Conflicts of interest: The authors declare no conflicts of interest regarding the materials or methods used in this study or the findings reported.

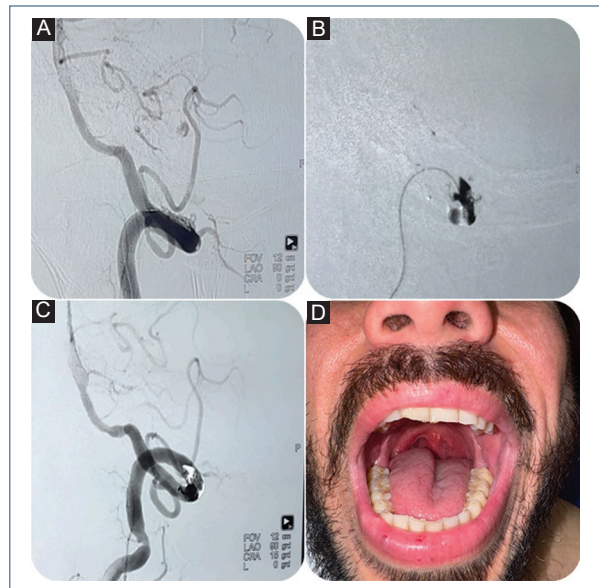


Figure 1. **A:** vertebral artery dural fistula. **B:** Onyx embolic agent deployment. **C:** balloon-assisted fistula repair in the vertebral artery. **D:** right cranial nerve IX and X paresis.

Brain volumes, cognitive dysfunction, and socioeconomic status in adults with and without Alzheimer's disease: an exploratory data analysis

Volúmenes encefálicos, disfunción cognitiva y estado socioeconómico en adultos con y sin enfermedad de Alzheimer: un análisis exploratorio de datos

Alberto Guevara-Tirado 

School of Human Medicine, Universidad Científica del Sur, Lima, Peru

Abstract

Background: Neurodegeneration in Alzheimer's dementia could be correlated with cognitive manifestations and socioeconomic factors. **Objective:** To analyze the correlation between intracranial and brain volume and the socioeconomic and cognitive states of adults with and without Alzheimer's disease (AD). **Method:** An analytical and cross-sectional study of secondary data from the open access imaging studies collection (OASIS), made up of 146 adults with dementia and 190 without dementia. The variables were sex, age, intracranial volume (eTIV), normalized brain volume (nWBV), educational level, socioeconomic status, mini mental health test (MMSE), and clinical dementia classification (CDR). The students' t-test, Mann-Whitney U, Spearman correlation, and multilayer perceptron were used. **Results:** Mean years of education, socioeconomic status, eTIV, and nWBV were lower in adults with AD. In adults without AD, nWBV was moderately correlated with age (Rho: -0.581) and socioeconomic status (Rho: 0.235). In adults with AD, nWBV was moderately correlated with age (Rho: -0.406), slightly with CDR (Rho: -0.285), moderately with MMSE (Rho: 0.401), while eTIV was moderately correlated with socioeconomic status (Rho: 0.467) and years of study (Rho: 0.409). The multilayer perceptron correctly predicted 91.50% of AD cases and correctly ruled out 74.80% of them. Its area under the curve was 0.862, indicating an acceptable classification model. **Conclusions:** In adults with AD, brain volume correlates with cognitive function, while eTIV correlates with socioeconomic status and years of study. Brain and intracranial volume, socioeconomic status, years of study, and sex were predictors of dementia using neural network analysis.

Keywords: Alzheimer disease. Cerebrum. Mental status and dementia tests. Socioeconomic factors. Correlation of data.

Resumen

Antecedentes: La neurodegeneración en la demencia de Alzheimer podría correlacionarse con manifestaciones cognitivas y factores socioeconómicos. **Objetivo:** Analizar la correlación entre volumen intracraneal y cerebral, con estados socioeconómicos y cognitivos de adultos con y sin enfermedad de Alzheimer (EA). **Método:** Estudio analítico y transversal, de datos secundarios de la colección de estudios de imágenes de acceso abierto (OASIS), conformado por 146 adultos con demencia y 190 sin demencia. Variables: sexo, edad, volumen intracraneal (eTIV), volumen cerebral normalizado (nWBV), nivel educativo, estado socioeconómico, Miniexamen de salud mental (MMSE), clasificación clínica de demencia (CDR). Se usó

Correspondence:

Alberto Guevara-Tirado
E-mail: albertoguevara1986@gmail.com

Date of reception: 12-11-2024
Date of acceptance: 13-11-2024
DOI: 10.24875/ANCE.M24000039

Available online: 24-04-2025
Arch Neurocién (Eng). 2025;30(4):163-171
www.archivosdeneurociencias.mx

3081-1562 / © 2024 Instituto Nacional de Neurología y Neurocirugía. Published by Permanyer. This is an open access article under the CC BY-NC-ND license (<http://creativecommons.org/licenses/by-nc-nd/4.0/>).

la prueba U de Mann-Whitney, correlación de Spearman y perceptrón multicapa. **Resultados:** Los promedios de años de educación, estado socioeconómico, eTIV y nWBV fueron menores en adultos con EA. En adultos sin EA, el nWBV se correlacionó moderadamente con la edad ($Rho: -0.581$) y el estado socioeconómico ($Rho: 0.235$). En adultos con EA, el nWBV se correlacionó moderadamente con la edad ($Rho: -0.406$), levemente con la CDR ($Rho: -0.285$) y moderadamente con el MMSE ($Rho: 0.401$), mientras que el eTIV se correlacionó moderadamente con el estado socioeconómico ($Rho: 0.467$) y años de estudio ($Rho: 0.409$). El perceptrón multicapa pronosticó correctamente el 91.50% de los casos de EA y descartó correctamente el 74.80% de ellos. Su área bajo la curva fue 0.862, lo que indica un modelo de clasificación aceptable. **Conclusiones:** En adultos con EA, el volumen cerebral se correlaciona con la función cognitiva, mientras que el eTIV con el estado socioeconómico y años de estudio. El volumen cerebral e intracraneal, estado socioeconómico, años de estudio y sexo fueron predictores de demencia mediante análisis de redes neuronales.

Palabras clave: Enfermedad de Alzheimer. Cerebro. Pruebas de estado mental y demencia. Factores socioeconómicos. Correlación de datos.

Introduction

Alzheimer's disease (AD) is a neurodegenerative disorder with a slow onset and progressive course, accounting for approximately 60 to 70% of dementia cases, affecting around 50 million people worldwide¹. It impacts short-term memory and causes progressive aphasia, disorientation, mood disturbances, loss of motivation, self-neglect, and behavioral changes². In advanced stages, the deterioration of functions leads to death³. The causes have been attributed to defects in acetylcholine synthesis⁴, beta-amyloid and tau proteinopathies⁵, with formation of paired helical filaments that create intracellular neurofibrillary tangles, affecting neuronal cytoarchitecture through microtubule disintegration and collapsing synaptic neurotransmission pathways⁶. It has also been proposed that AD represents an inverse cycle of fetal neurodevelopment⁷, as well as having infectious origins⁸.

The progressive loss of neurons and synapses in cortical and subcortical regions leads to atrophy of the hippocampus, frontal, parietal, and temporal lobes, cingulate gyrus, and brainstem⁹. The definitive diagnosis is post-mortem¹⁰; clinical diagnosis may present discrepancies (between 11 and 22%)¹¹, requiring a thorough evaluation of the past medical history, family background, neuropsychological studies, and the exclusion of brain disease or dementia subtypes¹². Risk factors include age¹³, genetics¹⁴, female sex, hypertension, head trauma, sedentary lifestyle, smoking¹⁵, and low cognitive reserve¹⁶.

Factors associated with early life stages that influence neuroplasticity, such as education, may affect brain anatomy in individuals with low cognitive reserve, as well as cognitive dysfunction. Therefore, the objective of this research was to analyze and compare the correlation between intracranial volume (eTIV) and

brain volume with socioeconomic and cognitive statuses in adults with and without Alzheimer's dementia. This will help determine the importance and potential impact of cognitive reserve (and postnatal neurodevelopmental phenotypic plasticity) on the brain architecture of older adults affected and unaffected by Alzheimer's dementia.

Methods

Study design and population

We conducted an analytical and cross-sectional study, derived from a preprocessed secondary source of the Open Access Series of Imaging Studies (OASIS) dataset, freely available to the international scientific community to facilitate future discoveries in basic and clinical neuroscience¹⁷. The study included a total of 336 contrast-free magnetic resonance imaging (MRI) data from adults aged 60 to 90, except for the "socioeconomic status" variable, where 19 data points were missing in the comparison of averages. The overall available population in the classified database was studied, so no sample calculation or randomization was performed. The characteristics of the database population can be observed in [table 1](#).

Variables and measurements

The variables were:

- Presence of AD, as a dichotomous variable (yes/no). AD was determined through neuropsychological tests and clinical diagnoses by neurologists, based on diagnostic criteria from the Diagnostic and Statistical Manual of Mental Disorders (DSM-5), which involve memory and learning decline, as well as at least one other cognitive domain (complex attention, executive

Table 1. Characteristics of the study population

Variable	n	Percentage
Sex		
Male	141	41.96%
Female	195	58.04%
Alzheimer		
Yes	146	43.50%
No	190	56.50%
Variable	Mean	Standard deviation
Age (years)	77.01	7.641
SES (score)	2.46	1.134
MMSE (score)	27.34	3.683
Years of study	14.60	2.876
CDR (score)	0.29	0.375
eTIV (mm ³)	1,488.129	176.13
nWBV (%)	0.73	0.037

CDR: Clinical Dementia Rating; eTIV: estimated total intracranial volume; MMSE: Mini-Mental State Examination; nWBV: normalized whole brain volume.

function, learning and memory, language, perception, motor and social cognition).

- Age (numerical variable, in years).
- Folstein Mini-Mental State Examination (MMSE) (numerical variable), a 30-point questionnaire to measure cognitive impairment and detect and estimate the severity of cognitive dysfunction, with validity and reliability for AD evaluation¹⁸. A score of 24 to 30 is considered normal, while scores < 24 indicate severe (≤ 9 points), moderate (10 to 18 points), or mild (19 to 23 points) cognitive impairment¹⁹.
- Clinical Dementia Rating (CDR), a scale quantifying the severity of dementia symptoms across stages, with a composite score ranging from 0 (none) to 3 (severe dementia symptoms)²⁰.
- Normalized whole brain volume (nWBV), the total sum of gray and white matter measured by MRI²¹, as a numerical variable.
- Estimated total intracranial volume (eTIV, numerical variable), the normalized volume within the skull, including the brain, meninges, and cerebrospinal fluid (CSF)²², evaluated by MRI and expressed in cubic millimeters (mm³).
- Both nWBV and eTIV were assessed using the Atlas scaling factor, a head size normalization technique based on an atlas to measure total eTIV and brain volume for comparison, classification, and prediction²³. Data related to the software used for estimation were not available.

- Years of education, as the total years of schooling completed.
- Socioeconomic status (SES), a combined socioeconomic measure of an individual or family's work experience and access to economic resources and social position, classified from 1 (low) up to 5 (high)²⁴.

Statistical analysis

After performing the Kolmogorov-Smirnov test, it was concluded that the distribution of the variables was non-normal, except for nWBV, so non-parametric statistical tests were conducted. The Mann-Whitney U test was used to compare the ranks of each variable based on the presence or absence of dementia. Spearman's correlation coefficient was used to determine the correlation between brain volumes and socioeconomic and cognitive factors in adults with and without AD, with a range of 0.1 up to 0.39 indicating weak correlation, 0.4 to 0.69 moderate correlation, and > 0.7 high correlation²⁵. Following the correlation results, the Bonferroni correction method was applied, resulting in an alpha value to reject the null hypothesis of < 0.005 after determining 10 comparisons. A multilayer perceptron artificial neural network was created to predict the presence of Alzheimer's dementia based on brain volume, intracranial volume, age, socioeconomic status, and years of education. The predictive capacity of the perceptron was estimated using the area under the curve, defined as excellent for a range of 0.90 to 1, acceptable for 0.80 to 0.89, fair for 0.70 to 0.79, and poor for 0.60 to 0.69²⁶. The total studied population (n = 317) was compared in a bivariate table based on the predicted values from the perceptron vs. confirmed AD results, with association measures such as Cramer's V coefficient, odds ratio (OR), prevalence ratio, and determination of sensitivity, specificity, and positive and negative predictive values. Data were collected and processed using SPSS v. 25™.

Ethical considerations

As this study was derived from a secondary source available in an open database, only data relevant to the research were accessed. Personal data were not accessible, as each participant's information had been coded, removing any data suggesting personal identity. The link to the OASIS project website is as follows: <https://www.oasis-brains.org/>.

Table 2. Comparison of ranks using the Mann-Whitney U Test for socioeconomic and brain volume variables in older adults with and without AD

Variable	n (yes - AD)	n (No - AD)	Average rank	Sum of ranks	p
Age (years)	146	190	162.51	23,726	0.321
Years of education (years)	146	190	140.94	20,577	< 0.001
Socioeconomics status (score)	127	190	147.36	27,997	0.004
MMSE (score)	146	190	93.38	13,446	< 0.001
eTIV (mm ³)	146	190	132.04	19,278	< 0.001
CDR (score)	146	190	262.8	38,369	< 0.001
nWBV (percentage)	146	190	132.04	19,278	< 0.001

CDR: Clinical Dementia Rating; EA: Alzheimer’s disease; eTIV: estimated total intracranial volume; MMSE: Mini-Mental State Examination; nWBV: normalized whole brain volume.

Results

When comparing groups with and without AD, there were no significant differences in age ($p = 0.321$). Significant differences were found in years of education ($p < 0.001$), where adults with AD had a lower average vs those without AD. In socioeconomic status, adults with AD had a lower average ($p = 0.004$). In MMSE and CDR, the averages were higher in adults with AD ($p < 0.001$ for both variables). Regarding eTIV and nWBV, adults with AD had lower averages vs. those without AD ($p < 0.001$ for both variables) (Table 2).

Spearman’s correlation analysis was performed, applying the Bonferroni correction method, where 10 comparisons (in groups with and without AD) were drawn, and the null hypothesis for each comparison was rejected if its significance level (p) was < 0.05 . In adults without AD, nWBV was moderately and negatively correlated with age (Rho: -0.581 ; $p < 0.001$) and weakly and positively correlated with socioeconomic status (Rho: 0.235 ; $p = 0.001$). In adults with AD, nWBV was moderately and negatively correlated with age (Rho: -0.406 ; $p < 0.001$), weakly and negatively correlated with clinical dementia rating (Rho: -0.285 ; $p = 0.001$), and moderately and positively correlated with MMSE (Rho: 0.401 ; $p < 0.001$), while eTIV was moderately and positively correlated with socioeconomic status (Rho: 0.467 ; $p < 0.001$) and years of education (Rho: 0.409 ; $p < 0.001$) (Table 3).

The neural network method (multilayer perceptron) resulted in 6 input layers, 5 hidden layers, and 2 output layers. In training, with 222 cases, it had a 25% incorrect prediction rate, and in testing, with 95 cases, a

Table 3. Correlation between brain volumes with socioeconomic and cognitive factors in adults with and without AD

Variable	Adults without AD		Adults with AD	
	nWBV	eTIV	nWBV	eTIV
Age				
Rho	-0.581	0.143	-0.406	-0.121
P	< 0.001	0.049	< 0.001	0.147
Socioeconomic status				
Rho	0.235	-0.149	-0.017	0.467
P	0.001	0.040	0.854	< 0.001
Years of education				
Rho	-0.153	0.115	0.062	0.409
P	0.035	0.112	0.460	< 0.001
CDR				
Rho	-0.015	0.135	-0.285	0.080
P	0.842	0.063	0.001	0.340
MMSE				
Rho	0.016	0.011	0.401	-0.103
P	0.827	0.876	< 0.001	0.217

CDR: Clinical Dementia Rating; AD: Alzheimer’s disease; eTIV: estimated total intracranial volume; MMSE: Mini-Mental State Examination; nWBV: normalized whole brain volume.

20% incorrect rate. The model in the testing stage correctly predicted 76% of AD cases correctly ruling out 91% of them. The variable that contributed most to the model was nWBV and the least contributing one was sex (Fig. 1). The area under the curve was 0.862, indicating that the model provided an acceptable classification and diagnostic model (Fig. 2).

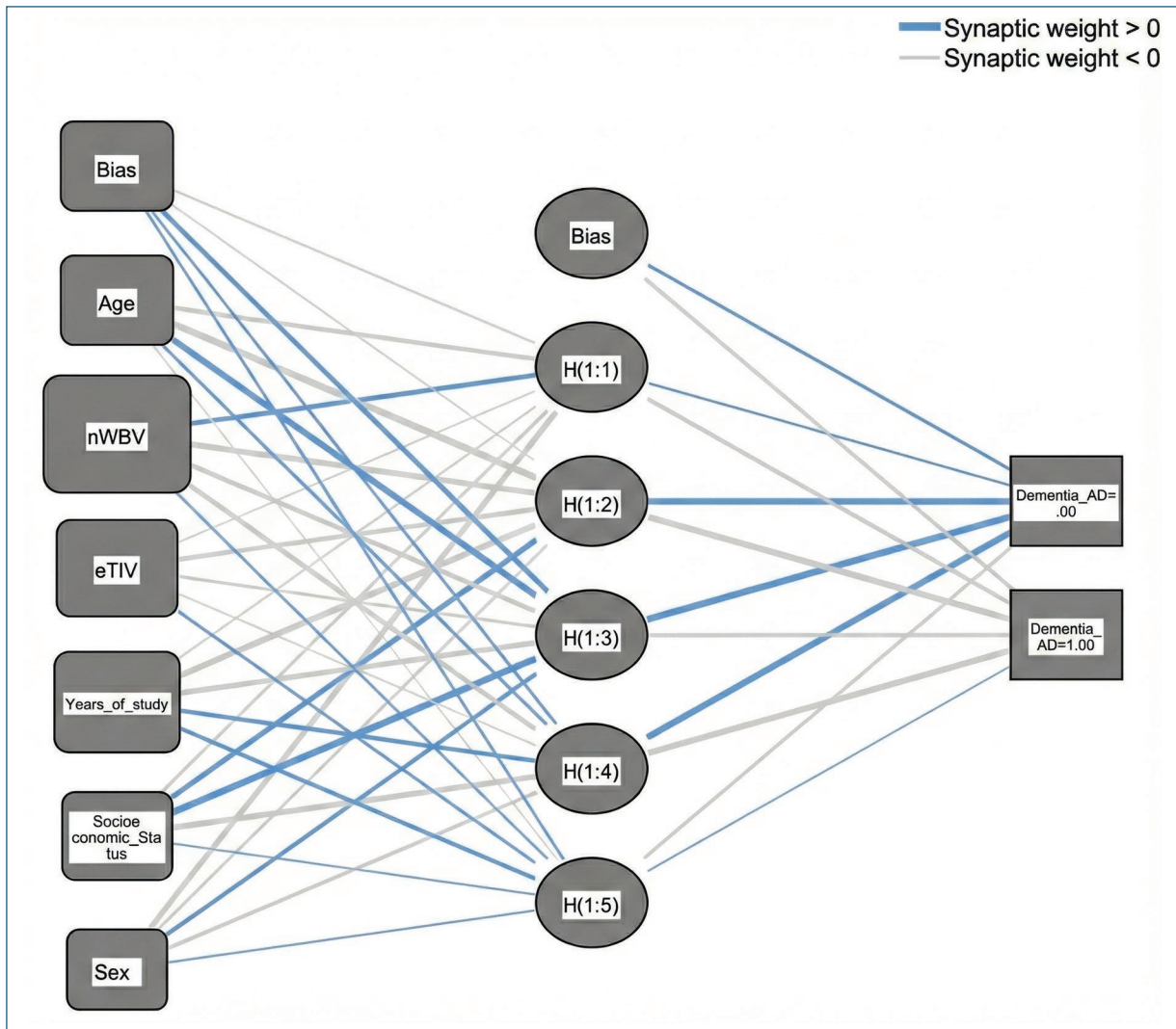


Figure 1. Multilayer perceptron artificial neural network structure for Alzheimer's dementia predictors. Hidden layer activation function: hyperbolic tangent. Output layer activation function: Softmax. EDUC: years of education; eTIV: estimated total intracranial volume; nWBV: normalized whole brain volume; SES: socioeconomic status.

A contingency table was created to compare the predicted values from the multilayer perceptron for the presence or absence of AD with the confirmed AD cases in the same population, combining the training and testing groups ($n = 317$). It was observed that predicted values and confirmed AD diagnoses matched in 91.50% of cases, while predicted negative cases matched 74.80% of confirmed negative cases (Table 4).

An analysis of the previous table showed that the association between predicted AD cases using the multilayer perceptron and confirmed AD cases was high ($V: 0.564$). Patients predicted by the perceptron had a 32.15 times higher probability (OR) of confirmed AD diagnosis than those predicted as negative by the perceptron, and a 3.63 times higher frequency (prevalence ratio). The perceptron model had a sensitivity of 51%,

specificity of 97%, and high positive and negative predictive values (PPV: 92%, NPV: 97%) (Table 5).

Discussion

The mean MMSE score was normal in adults without AD, while it was in the moderate-to-severe range in adults with AD. Differences were found in years of education, with fewer years in adults with AD, aligning with the notion that more years of education increase cognitive reserve, preserving and compensating for cognitive deficits, delaying or preventing the onset of dementia²⁷. It was also observed that nWBV was lower in adults with AD, consistent with imaging and post-mortem modalities showing brain atrophy with loss of gyri and sulci, prominently in the temporal and parietal

Table 4. Comparison of matches between the total predicted cases of AD by multilayer perceptron and the total confirmed ad cases ($p < 0.001$)

Predicted values using neural network vs. observed values		Patients with confirmed AD diagnosis	
Predicted AD value via multilayer perceptron	Total = 317	AD	No AD
	AD (n = 71)	65 (91.50%)	6 (8.50%)
	No AD (n = 246)	62 (25.20%)	184 (74.80%)

AD: Alzheimer's disease.

Table 5. Association measures, probability, and diagnostic capacity between total predicted AD cases via multilayer perceptron and the total confirmed AD cases

Performance metrics	V	OR	RR	S	Sp	PPV	NPV
AD perceptron - Confirmed AD	0.564	32	3.63	51%	97%	92%	97%

OR: odds ratio; RP: risk ratio; S: sensitivity; Sp: specificity; VPP: positive predictive value; VPN: negative predictive value; V: Cramér's V coefficient; AD: Alzheimer's disease.

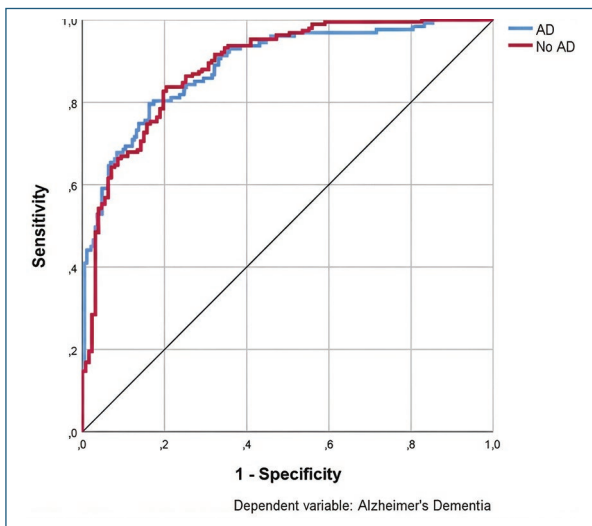


Figure 2. Area under the curve of the multilayer perceptron model for adults with Alzheimer's disease.

lobes, parts of the cortex, and cingulate gyrus, attributed to progressive acetylcholine deficiency and underlying proteinopathy²⁸. Currently, MRI use in AD focuses mainly on hippocampal-predominant brain atrophy evaluation, which, however, has limited specificity. Brain volumetry is proposed for assessing clinical status and progression of AD, as well as understanding underlying disease mechanisms related to volume reduction due to progressive loss of neuronal connections and cellular dysfunction²⁹.

Similarly, adults with AD had a lower average socioeconomic status, which is consistent with observations

suggesting that lower socioeconomic status (which may be related to cognitively less stimulating work activities), as well as lower income (which could predispose to less healthy lifestyles), are factors that increase dementia prevalence in this patient group³⁰. These results showed that differences between those affected and unaffected by AD include aspects that expand neurobiological concepts to socioeconomic and educational factors.

In the correlation analysis for adults with AD, nWBV correlated with clinical dementia rating and MMSE. The relationship between brain volume and cognition was studied by Royle et al., who investigated the association between brain imaging biomarkers (including brain volumes) and cognitive ability measures in 73-year-old adults, finding a positive relationship between white and gray matter and cognitive function, with anterior brain volume (from childhood and adulthood) being a predictor of current cognitive reserve³¹. Dinomais et al. studied the possible anatomical brain correlation with MMSE in individuals older than 60 with and without cognitive impairment, finding that MMSE was associated with gray matter, predominantly in the limbic system³². Results suggest that the correlation with cognitive dysfunction severity may predominantly involve gray matter, responsible for information processing, and white matter, which conducts and sends signals, with morphological changes such as demyelination observed in the latter from preclinical stages of Alzheimer's, preceding beta-amyloid and tau accumulation³³. Therefore,

imaging modalities, in addition to their utility for differential diagnosis, could be a potential predictor of cognitive functional decline.

eTIV in adults with AD was lower than in adults without AD and was moderately and positively correlated with socioeconomic status and years of education. Hou et al., in a study investigating associations between lifestyles and AD biomarkers in CSF, found lower levels of tau and beta-amyloid protein in adults with healthy lifestyles³⁴. In this regard, while healthy lifestyles reduce the risk of developing AD, it can be conjectured that the decrease in eTIV, which includes white and gray matter, meninges, and CSF, is influenced by lifestyles related to work activity and education via CSF, as CSF flow depends on cardiac, respiratory, and circadian rhythms³⁵, affecting functions such as waste removal, toxic substance elimination, and internal pressure stabilization. Therefore, imbalances associated with stressful lifestyles, generally associated with low economic resources and educational levels, would alter these oscillations, affecting CSF homeostasis in AD patients, potentially considered as a possible pathway in the progressive development of AD.

The mechanisms by which reduced eTIV is related to AD progression include changes to blood-brain barrier components (pericytes, astrocytes, vascular endothelial cells, and tight junctions), generating neuroinflammation, oxidative stress, and increased secretases promoting beta-amyloid formation³⁶. Although blood-brain barrier weakening is associated with age, it is also associated with the accumulation of neurotoxic products in the blood, causing progressive barrier weakening, with subsequent access of neurotoxic proteins such as fibrin, bacteria-like *Chlamydomonas pneumoniae*, viruses such as herpes zoster, metals like lead and aluminum, among others³⁷, increasing AD risk and thus opening exposure to this disease through the entry of exogenous factors.

Considering both brain volumes in adults with AD, it is possible to affirm that brain volume, with emphasis on gray matter, correlates with current cognitive dysfunction, making it a potential predictor of cognitive decline, while eTIV correlates with factors related to activities developed in stages prior to the patients' current condition, meaning past lifestyles would predict the severity of eTIV involuntarily changes, associated with the homeostatic equilibrium medium of CSF. The importance of the studied variables was verified in the neural network analysis, where eTIV and nWBV had very high importance in predicting potential AD cases.

The predictive capabilities of the variables included in the perceptron are based on foundations consistent with structural and functional changes due to persistent corticosteroid release and response influenced by chronic exposure to environmental and socioeconomic stressors, generating dysregulation of the hypothalamic-pituitary-adrenal axis associated with decreased brain volume and neuroplasticity, mainly (but not limited to) in areas like the amygdala and hippocampus. These effects are attributed to chronic corticosteroid elevation (from multifactorial stress) reducing brain-derived neurotrophic factor expression, as well as epigenetic mechanisms affecting neuronal and glial plasticity. Corticosteroids, along with catecholamines, are relevant for behavioral adaptation to stress and preservation of significant emotional information, through synaptic regulation and plasticity, facilitating initial encoding of systemic memory in the hippocampus and later in the neocortex, and their persistent elevations have been associated with impaired synaptic plasticity and dendritic atrophy, compromising neuronal survival to various damaging factors and neuronal death, especially in the hippocampus, which has higher receptor sensitivity to corticosteroids, making it particularly vulnerable to neuroinflammation, neurodegeneration up to the subgranular niche, and aberrant neuronal network formation³⁸.

In this regard, the effect induced by socioeconomic status and lower educational level as predictors of low cognitive reserve and AD is associated, in addition to chronic stressors linked to economic deprivation, with lower linguistic, social, and cognitive stimulation, which has been associated with reduced cortical development of the left hemisphere, amygdala, prefrontal cortex, and hippocampus from early life stages to early adulthood³⁹. Sex is a predictive factor, especially due to sex differences in disease presentation, with AD being more frequent in women. Several factors intervene: the drop in estrogen levels generates bioenergetic uncoupling during perimenopause and a hypometabolic state that produces dysfunctions in metabolic, inflammatory, and sensory processing molecular pathways⁴⁰, including the protective effect of estrogen by generating vesicles containing amyloid precursor protein in the Golgi apparatus, promoting beta-amyloid delivery to the cell surface, reducing its intracellular concentrations; similarly, it reduces hyperphosphorylated tau, thus increasing dephosphorylated tau⁴¹. Other differences include the experimentally observed effect of follicle-stimulating hormone on increased beta-amyloid and tau deposition on cortical

and hippocampal neurons, sex-specific immune responses (intensified microglial responses in women have been observed), increased proteostasis predominantly of beta-amyloid and hyperphosphorylated tau, microbiome differences, sociocultural factors regarding access to education, sex differences, and greater longevity, among others⁴².

The limitations of this study were related to the source, being a secondary database, so the information could present biases. Additionally, the effectiveness of the multilayer perceptron model was lower than expected for predicting Alzheimer's dementia, although its main utility in this research was to determine if the variables used were predictors of the disease, rather than creating a clinically useful predictive model, as parameters like brain and intracranial volumes are highly costly, requiring imaging tests, with clinical diagnosis being much more cost-effective and efficient.

In conclusion, in adults with AD, nWBV correlates with cognitive function, while eTIV correlates with socioeconomic status and years of education. Using neural networks, brain and intracranial volume, socioeconomic status, years of education, and sex were predictors of AD. Imaging modalities could be predictors of cognitive dysfunction in AD patients. Further studies are needed to determine the influence and pathophysiological mechanisms of each lifestyle-related factor on eTIV anatomy in AD patients. Additionally, the use of simple neural networks like multilayer perceptrons can complement clinical decisions made by neurologists regarding the diagnosis or exclusion of this disease.

Funding

This research has not received any specific grants from public, commercial, or for-profit agencies.

Conflicts of interest

The author declares that he has no conflicts of interest.

Ethical considerations

Protection of people and animals. The author declares that no experiments were conducted on humans or animals for this research.

Confidentiality, informed consent, and ethical approval. The study does not involve personal patient data and does not require ethical approval. The SAGER guidelines do not apply.

Statement on the use of artificial intelligence. The author declares that no generative artificial intelligence was used in the writing of this manuscript.






References

- Domingues R, Pereira C, Cruz MT, Silva A. Therapies for Alzheimer's disease: a metabolic perspective. *Mol Genet Metab.* 2021;132(3):162-72.
- Kim J, Jang H, Park YH, Youn J, Seo SW, Kim HJ, et al. Motor symptoms in early- versus late-onset Alzheimer's disease. *J Alzheimers Dis.* 2023;91(1):345-54.
- 2023 Alzheimer's disease facts and figures. *Alzheimers Dement.* 2023;19(4):1598-695.
- Terry AV Jr, Buccafusco JJ. The cholinergic hypothesis of age and Alzheimer's disease-related cognitive deficits: Recent challenges and their implications for novel drug development. *J Pharmacol Exp Ther.* 2003;306(3):821-7.
- Sharma C, Kim SR. Linking oxidative stress and proteinopathy in Alzheimer's disease. *Antioxidants (Basel).* 2021;10(8):1231.
- DeTure MA, Dickson DW. The neuropathological diagnosis of Alzheimer's disease. *Mol Neurodegener.* 2019;14(1):32.
- Xie C, Fong MC-M, Ma MK-H, Wang J, Wang WS. The retrogenesis of age-related decline in declarative and procedural memory. *Front Psychol.* 2023;14:1212614.
- Vigasova D, Nemerout M, Liskova B, Damborsky J. Multi-pathogen infections and Alzheimer's disease. *Microb Cell Fact.* 2021;20(1):25.
- Chauveau L, Kuhn E, Palix C, Felisatti F, Ourry V, de La Sayette V, et al. Medial temporal lobe subregional atrophy in aging and Alzheimer's disease: A longitudinal study. *Front Aging Neurosci.* 2021;13:750154.
- Handen BL, Christian BT. PET imaging in Down syndrome and Alzheimer's disease. En: *The Neurobiology of Aging and Alzheimer Disease in Down Syndrome.* Elsevier; 2022. pp. 173-92.
- Hazan J, Liu KY, Fox N, Howard R. Advancing diagnostic certainty in Alzheimer's disease: A synthesis of the diagnostic process. *J Alzheimers Dis.* 2023;94(2):473-82.
- Dubois B, Villain N, Frisoni GB, Rabinovici GD, Sabbagh M, Cappa S, et al. Clinical diagnosis of Alzheimer's disease: recommendations of the International Working Group. *Lancet Neurol.* 2021;20(6):484-96.
- Corrada MM, Brookmeyer R, Paganini-Hill A, Berlau D, Kawas CH. Dementia incidence continues to increase with age in the oldest old: The 90+ study. *Ann Neurol.* 2010;67(1):114-21.
- Andrade-Guerrero J, Santiago-Balmaseda A, Jeronimo-Aguilar P, Vargas-Rodríguez I, Cadena-Suárez AR, Sánchez-Garibay C, et al. Alzheimer's disease: An updated overview of its genetics. *Int J Mol Sci.* 2023;24(4):3754.
- Armstrong R. Risk factors for Alzheimer's disease. *Folia Neuropathol.* 2019;57(2):87-105.
- Lee DH, Seo SW, Roh JH, Oh M, Oh JS, Oh SJ, et al. Effects of cognitive reserve in Alzheimer's disease and cognitively unimpaired individuals. *Front Aging Neurosci.* 2022;13:784054.
- OASIS brains. Open Access Series of Imaging Studies [Internet]. Washington University School of Medicine in St. Louis, OASIS [cited January 29, 2024]. Available in: <https://www.oasis-brains.org>
- Gallegos M, Morgan ML, Cervigni M, Martino P, Murray J, Calandra M, et al. 45 Years of the mini-mental state examination (MMSE): a perspective from ibero-america. *Dement Neuropsychol.* 2022;16(4):384-7.
- Mini-Mental State Examination (MMSE). Stroke Engine [cited January 29, 2024]. Available in: <https://strokengine.ca/en/assessments/mini-mental-state-examination-mmse>
- Huang H-C, Tseng Y-M, Chen Y-C, Chen P-Y, Chiu H-Y. Diagnostic accuracy of the Clinical Dementia Rating Scale for detecting mild cognitive impairment and dementia: a bivariate meta-analysis. *Int J Geriatr Psychiatry.* 2021;36(2):239-51.
- Kijonka M, Borys D, Psiuk-Maksymowicz K, Gorczewski K, Wojcieszek P, Kossowski B, et al. Whole brain and cranial size adjustments in volumetric brain analyses of sex- and age-related trends. *Front Neurosci.* 2020;14:278.
- Malone IB, Leung KK, Clegg S, Barnes J, Whitwell JL, Ashburner J, et al. Accurate automatic estimation of total intracranial volume: A nuisance variable with less nuisance. *Neuroimage.* 2015;104:366-72.
- Buckner RL, Head D, Parker J, Fotenos AF, Marcus D, Morris JC, et al. A unified approach for morphometric and functional data analysis in young, old, and demented adults using automated atlas-based head size normalization: reliability and validation against manual measurement of total intracranial volume. *Neuroimage.* 2004;23(2):724-38.
- Vincent K, Sutherland JM, editors. A review of methods for deriving an index for socioeconomic status in British Columbia [Internet]. Vancouver: UBC Centre for Health Services and Policy Research; 2013 [accessed December 9, 2024]. Available in: <https://www.healthcarefunding.ca/files/2013/04/Review-of-Methods-for-SES-Index-for-BC.pdf>

25. Akoglu H. User's guide to correlation coefficients. *Turk J Emerg Med.* 2018;18(3):91-3.
26. Nahm FS. Receiver operating characteristic curve: overview and practical use for clinicians. *Korean J Anesthesiol.* 2022;75(1):25-36.
27. Rosselli M, Uribe IV, Ahne E, Shihadeh L. Culture, ethnicity, and level of education in Alzheimer's disease. *Neurotherapeutics.* 2022;19(1):26-54.
28. Traini E, Carotenuto A, Fasanaro AM, Amenta F. Volume analysis of brain cognitive areas in Alzheimer's disease: Interim 3-year results from the ASCOMALVA trial. *J Alzheimers Dis.* 2020;76(1):317-29.
29. Giorgio A, De Stefano N. Clinical use of brain volumetry. *J Magn Reson Imaging.* 2013;37(1):1-14.
30. Lai KY, Webster C, Kumari S, Gallacher JEJ, Sarkar C. The associations of socioeconomic status with incident dementia and Alzheimer's disease are modified by leucocyte telomere length: a population-based cohort study. *Sci Rep.* 2023;13(1):1-13.
31. Royle NA, Booth T, Valdés Hernández MC, Penke L, Murray C, Gow AJ, et al. Estimated maximal and current brain volume predict cognitive ability in old age. *Neurobiol Aging.* 2013;34(12):2726-33.
32. Dinomais M, Celle S, Duval GT, Roche F, Henni S, Bartha R, et al. Anatomic correlation of the mini-mental state examination: A voxel-based morphometric study in older adults. *PLoS One.* 2016;11(10):e0162889.
33. Nasrabady SE, Rizvi B, Goldman JE, Brickman AM. White matter changes in Alzheimer's disease: a focus on myelin and oligodendrocytes. *Acta Neuropathol Commun.* 2018;6(1):22.
34. Hou X-H, Xu W, Bi Y-L, Shen X-N, Ma Y-H, Dong Q, et al. Associations of healthy lifestyles with cerebrospinal fluid biomarkers of Alzheimer's disease pathology in cognitively intact older adults: the CABLE study. *Alzheimers Res Ther.* 2021;13(1):81.
35. Vijayakrishnan Nair V, Kish BR, Inglis B, Yang H-CS, Wright AM, Wu Y-C, et al. Human CSF movement influenced by vascular low frequency oscillations and respiration. *Front Physiol.* 2022;13:940140.
36. Cai Z, Qiao P-F, Wan C-Q, Cai M, Zhou N-K, Li Q. Role of blood-brain barrier in Alzheimer's disease. *J Alzheimers Dis.* 2018;63(4):1223-34.
37. Alkhalifa AE, Al-Ghraiyyah NF, Odum J, Shunnarah JG, Austin N, Kad-doumi A. Blood-brain barrier breakdown in Alzheimer's Disease: Mechanisms and targeted strategies. *Int J Mol Sci.* 2023;24(22):16288.
38. Gulyaeva NV. Glucocorticoids orchestrate adult hippocampal plasticity: Growth points and translational aspects. *Biochemistry (Mosc).* 2023;88(5):565-89.
39. Brito NH, Noble KG. Socioeconomic status and structural brain development. *Front Neurosci.* 2014;8:103217.
40. Brinton RD, Yao J, Yin F, Mack WJ, Cadenas E. Perimenopause as a neurological transition state. *Nat Rev Endocrinol.* 2015;11(7):393-405.
41. Yun J, Yeo IJ, Hwang CJ, Choi D-Y, Im H-S, Kim JY, et al. Estrogen deficiency exacerbates A β -induced memory impairment through enhancement of neuroinflammation, amyloidogenesis and NF- κ B activation in ovariectomized mice. *Brain Behav Immun.* 2018;73:282-93.
42. Lopez-Lee C, Torres ERS, Carling G, Gan L. Mechanisms of sex differences in Alzheimer's disease. *Neuron.* 2024;112(8):1208-21.

Possible involvement of dorsal hippocampal G-protein coupled receptor 55 (GPR55) in nicotine-induced conditioned place preference in rats

Posible participación del receptor acoplado a proteínas G 55 (GPR55) del hipocampo dorsal en la preferencia de lugar condicionada inducida por nicotina

Oliver A. Colis-Arenas¹ , Angélica Muñoz-Pelayo¹ , Carlos H. López-Lariz² , Jesús Chávez-Reyes² , and Bruno A. Marichal Cancino^{2*} 

¹Department of Medicine, Health Sciences Center; ²Department of Physiology and Pharmacology, Center for Basic Sciences. Universidad Autónoma de Aguascalientes, Aguascalientes, Ags., Mexico

Abstract

Background: The G-protein coupled receptor 55 (GPR55) is a cannabinoid/lysophospholipid target expressed in several tissues in mammals, including the central nervous system (CNS). Its actions in CNS are only partially known and include anxiety, spatial memory, reward, and pain. A recent study reported that systemic O-1602 (a GPR55 agonist) blocked the nicotine-induced conditioned place preference (CPP), but the knockdown of GPR55 in the nucleus accumbens did not modify the actions of O-1602, so its site of action remains obscure. GPR55 is expressed significantly in the dorsal hippocampus, a structure involved in the context-association to drugs-reward. **Objective:** To preliminary analyze the potential participation of dorsal-hippocampal GPR55 in the nicotine-induced CPP. **Method:** Male Wistar rats were implanted in dorsal hippocampus to receive: (i) vehicle (dimethyl sulfoxide 10%); (ii) ML184 (0.48 nmol; GPR55 agonist); or (iii) CID16020046 (1.16 nmol; GPR55 antagonist) during the conditioning phase in the nicotine-mediated CPP paradigm. **Results:** Animals from the vehicle group exhibited an increased time in the nicotine-paired chamber compared with its baseline ($p < 0.05$). In contrast, both ML184 and CID16020046 prevented the nicotine-induced CPP ($p > 0.05$). **Conclusion:** Under our experimental conditions, pharmacological manipulation of GPR55 in the dorsal hippocampus prevented the nicotine-induced CPP due to mechanisms that remain to be identified.

Keywords: G-protein coupled receptor 55. Conditioned place preference. Nicotine. Dorsal hippocampus. Brain reward.

Resumen

Antecedentes: El receptor acoplado a proteínas G 55 (GPR55) puede interactuar con cannabinoides y lisofosfolípidos. Se expresa en diversos tejidos en los mamíferos, incluyendo el sistema nervioso central (SNC). Sus acciones en el SNC se conocen parcialmente e incluyen efectos en ansiedad, memoria espacial, recompensa y dolor. Un estudio reciente reportó que la administración sistémica de O-1602 (agonista GPR55) inhibe la preferencia de lugar condicionada (CPP) inducida por nicotina, pero el silenciamiento del GPR55 en el núcleo accumbens no modifica las acciones del O-1602, por lo que su sitio de acción se desconoce. El GPR55 se expresa significativamente en el hipocampo dorsal, una estructura involucrada en la asociación contextual de la recompensa por drogas. **Objetivo:** Analizar de manera preliminar la participación potencial

*Correspondence:

Bruno A. Marichal Cancino
E-mail: bruno.marichal@edu.uaa.mx

Date of reception: 25-09-2024
Date of acceptance: 22-01-2025
DOI: 10.24875/ANC.24000006

Available online: 24-04-2025
Arch Neurocién (Eng). 2025;30(4):172-179
www.archivosdeneurociencias.mx

3081-1562 / © 2025 Instituto Nacional de Neurología y Neurocirugía. Published by Permanyer. This is an open access article under the CC BY-NC-ND license (<http://creativecommons.org/licenses/by-nc-nd/4.0/>).

del GPR55 en la CPP inducida por nicotina. **Método:** Ratas Wistar macho fueron canuladas en el hipocampo dorsal para recibirla con: (a) vehículo (DMSO10%); (b) ML184 (0.48 nmol; GPR55 antagonista), o (c) CID16020046 (1.16 nmol; GPR55 antagonist) durante la fase de condicionamiento en el CPP mediado por nicotina. **Resultados:** Los animales a los cuales se les administró con vehículo pasaron más tiempo en la cámara emparejada con nicotina en comparación con la línea base ($p < 0.05$). Por el contrario, ML184 y CID16020046 previnieron la CPP inducida por la nicotina ($p > 0.05$). **Conclusión:** Bajo nuestras condiciones experimentales, la manipulación farmacológica del GPR55 en el hipocampo dorsal previno la CPP inducida por nicotina por mecanismos aún no identificados.

Palabras clave: GPR55. Preferencia de lugar condicionado. Nicotina. Hipocampo dorsal. Recompensa del cerebro.

Significance statement

Our findings support previous reports that claim the participation of GPR55 in the central nervous system in the reinforcing actions of nicotine and propound GPR55 in the dorsal hippocampus as one of the possible sites of action.

Introduction

The conditioning place preference (CPP) is a classic paradigm to evaluate the potential of drugs to promote behavior induced by reward through the experience in two different sensorial contexts, one of them paired to a drug and the other one paired to its vehicle¹. The previous studies have analyzed and concluded that the dorsal hippocampus (a key brain area involved in contextual memories and place location recognition) is participating in establishing CPP^{2,3}. For this reason, the dorsal hippocampus (particularly the CA1 structure) represents an interesting brain-associative area in which physiology may allow us to understand the neurocircuits involved in the drug-seeking/intake phenomena⁴⁻⁶. Moreover, the hippocampus, the amygdala, and the ventral striatum receive dopamine from the tegmental ventral area; this circuitry represents the mesolimbic system, whose functions include brain reward, motivation, eating behavior, blood flow control, and others⁷⁻⁹. The function of the mesolimbic system is highly modulated by the endocannabinoid system¹⁰.

The hippocampal functions are modulated by (i) classic mediators such as catecholamines¹¹ and (ii) non-classic mediators, e.g., opioids, cannabinoids, etc.^{12,13}. From the non-classic mediators, cannabinoids reach the G protein-coupled receptor 55 (GPR55), which has a complex pharmacology that includes a biased agonism through lysophospholipids (e.g., LPI) and cannabinoids^{14,15}. In addition to several peripheral tissues, GPR55 is highly expressed in the central nervous system and has been related to pain, anxiety,

memory, and brain reward¹⁶⁻²¹. Interestingly, this receptor may exert a functional pivotal role in some brain areas, such as the striatum²² and hippocampus¹⁹. To support the above notion, in a Parkinson's preclinical model induced through 6-hydroxydopamine, both LPI (an endogenous GPR55 agonist) and ML193 (a synthetic antagonist) improved locomotion²². Likewise, injections of both LPI and CID1602046, but not its vehicle, impaired spatial memory in the Barnes maze¹⁹. In a previous study, we reported that both (i.c.v.) ML184 (a GPR55 agonist) and ML193 (a GPR55 antagonist) prevented the nicotine-mediated CPP²¹. Another interesting independent study concluded that GPR55 in the ventral striatum could partially explain the preventive actions of O-1602 (GPR55 agonist) against the nicotine-induced CPP²³. Nevertheless, the preventive actions of O-1602 on nicotine-induced CPP remained after GPR55 receptor knockdown in the ventral striatum by selective lentiviral shRNA²³, suggesting the participation of other brain areas. Hence, the present study was set up to investigate the pharmacological actions of the GPR55-related synthetic drugs ML-184 (agonist) and CID16020046 (antagonist) in the dorsal hippocampus on nicotine-induced CPP in rats.

Materials and methods

Animals

Thirty-four male Wistar rats (250-300 g) were obtained from the vivarium facilities of the *Universidad Autónoma de Aguascalientes*. Animals were housed for habituation for three days at a constant $23 \pm 1^\circ\text{C}$ temperature, humidity 28-35%, and a 12 h light/dark cycle starting lights at 10:00 am. Water and food were added *ad libitum*. All experimental procedures were approved by the Institutional Ethics Committee (CEADI-UAA) and performed in harmony with the Mexican guidelines for animal care NOM-062-ZOO-1999 referred to as "Technical specifications for the production, use and care of laboratory animals." Our study adhered to the ARRIVE

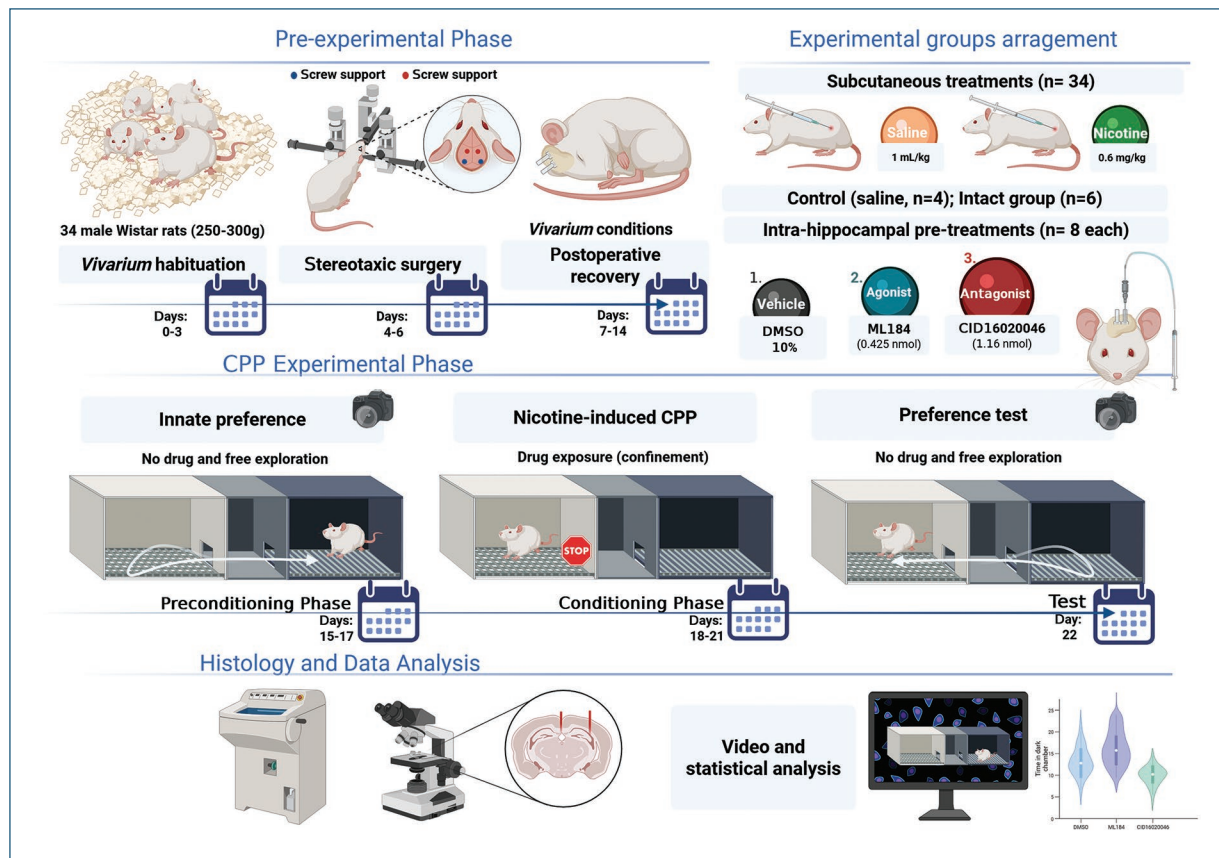


Figure 1. Experimental design scheme. Created in <https://BioRender.com>

guidelines for preclinical animal research as outlined by the EQUATOR Network, the Guide for the Care and Use of Laboratory Animals in the USA²⁴, and the Directive 2010/63/Eu of the European Parliament and of the Council of September 22, 2010, on the protection of animals used for scientific purposes (available at: <http://eur-lex.europa.eu/LexUriServ/LexUriServ.do?uri=OJ:L:2010:276:0033:0079:en:PD>).

Drugs

CID16020046 ("4-[4-(3-hydroxyphenyl)-3-(4-methylphenyl)-6-oxo-1,4-dihydropyrrolo[3,4-d] pyrazol-5-yl] benzoic acid"), ML184 (CID2440433, "3-[4-(2,3-dimethylphenyl) piperazine-1-carbonyl]-N, N-dimethyl-4-(pyrrolidin-1-yl) benzene-1-sulfonamide"), and nicotine were obtained from Sigma-Aldrich®. Nicotine (0.6 mg/kg) was prepared in saline solution (SS, 0.9% w/v NaCl) and injected (s.c.) in a volume of 0.3 mL, ML184 (0.425 nmol; each side in 1 μ L) and CID16020046 (1.16 nmol; each side in 1 μ L) working solutions were diluted in dimethyl sulfoxide (DMSO) 10% and (SS, 0.9% w/v). Concentrations of compounds

referred to in this text correspond to their free base. Fresh solutions were prepared on each experimental day.

Stereotaxic surgery

Rats were anesthetized with a Zoletil® 50 (tiletamine 125 mg + zolazepam 125 mg) + xylazine cocktail (35 mg/kg + 8 mg/kg, respectively) in a volume of 1 mL/kg i.p. Under deep anesthesia, animals were placed in a stereotaxic frame, and two cannulas (22G \times 10 mm) were implanted bilaterally into the dorsal hippocampus, where compounds were injected. Intra-hippocampal cannulation coordinates were AP: -3.24 mm, ML: ± 1.6 mm, and DV: 2.8²⁵. Two stainless-steel screws attached to the skull and a solidified dental acrylic layer helped to fix the cannulas during all experimentation periods. After surgery, animals recovered individually housed and allowed to heal for 7 days under the abovementioned *vivarium* conditions. In addition, animals received Neomycin-ointment (Brosin®) and Ketoprofen 2.5 mg/kg s.c. for 3 post-surgery days (Fig. 1).

Intradorsal-hippocampus administration of the drugs

An injector (30 G × 11 mm) connected through Tygon® tubing (0.25 mm × 150 mm) to a Hamilton® 10 µL syringe was gently inserted into the cannula, and 1 µL of each pre-treatment was administered (0.018 µL/s) bilaterally during 1 min by a Syringe Pump Mod. 35 s (Sage Instruments™).

Experimental groups

To analyze the nicotine-induced CPP, the 34 rats were randomly assigned to the following groups: (i) intact rats (which received treatment with 0.6 mg/kg of nicotine during the conditioning phase; n = 6); (ii) control-group (which received an intradorsal hippocampus pretreatment of DMSO 10%; n = 4); (iii) a nicotine group (which received an intradorsal hippocampus pretreatment of DMSO 10% and treatment with 0.6 mg/kg of nicotine during the conditioning phase; n = 8); (iv) a GPR55-agonist group (which received an intradorsal hippocampus pretreatment of 0.48 nmol of ML-184 and treatment with 0.6 mg/kg of nicotine during the conditioning phase; n = 8); and (v) a GPR55-antagonist group (which received an intradorsal hippocampus pretreatment of 1.16 nmol of CID1602046 and treatment with 0.6 mg/kg of nicotine during the conditioning phase; n = 8). All groups shared temporal synchronicity in the experimental procedures²⁶.

Conditioned place preference paradigm (CPP)

THE CPP APPARATUS

Unforced choice CPP paradigm chamber comprises two acrylic compartments (30 × 30 × 45 cm) connected through a cramped chamber (14.5 × 13 × 30 cm) with two vertical sliding guillotines that facilitate or block the access to both external compartments (Fig. 1). External chambers differ on visual and tactile cues, resulting in one compartment more comfortable to the animal than the other. The left chamber had white-colored walls and a flat floor, whereas the right chamber had black and white vertical lines on two walls and diagonally disposed black and white lines on the other two. The CPP paradigm room conditions were red light illumination and minimal sound stimuli.

PRECONDITIONING PHASE

The CPP protocol was performed as previously described by²¹, in which, in the preconditioning stage, the rat was placed in the central compartment and allowed to freely explore the CPP-apparatus for 15 min for 3 days (Fig. 1). Sessions were videotaped with a webcam (Logitech Mod. C922PRO) at 1280 × 720 px and 30 fps. The time spent in each compartment was measured for 3 days, and the means were used to determine the natural preference of each animal for a specific chamber.

CONDITIONING PHASE

Animals were exposed to the CPP environments in a counterbalance scheme. Always considering the natural preference, animals were randomly injected with SS or nicotine in the morning (10:00 am) and confined for 30 min in (i) the preferred chamber (saline-paired) or (ii) the non-preferred chamber (nicotine-paired). Six hours later, the opposite treatment was injected, and the rat was confined for 30 min in the opposite chamber. This protocol was repeated for four consecutive days (Fig. 1); however, the order of the treatments was also counterbalanced, so the rats that received saline during the morning on the previous day received nicotine first on the second day and so on alternatively.

CPP TEST

A CPP test was carried out on the 22nd day (Fig. 1). No treatment/pre-treatment was administrated on the CPP test day. Each rat was placed into the central compartment and allowed to navigate into the CPP compartments freely. Experimental videos were saved after 15 min. Significant increments in time spent in the nicotine-paired test versus during the preconditioning phase were considered a reinforcing effect. The influence of ML184 and CID16020046 on the reinforcing action of nicotine was subsequently evaluated.

Histology

Nissl staining protocol was performed to evaluate the correct placement of cannulas (Fig. 1). Brains were extracted from perfused rats with SS and *p*-formaldehyde (4% w/v), brains once collected were refrigerated 1 week at 4°C followed by an additional week on sucrose (20% w/v). Brains were coronally sectioned, positioned on the cryostat for 70 µm cutting, placed on a glass slide for Nissl stain, and finally, cannula

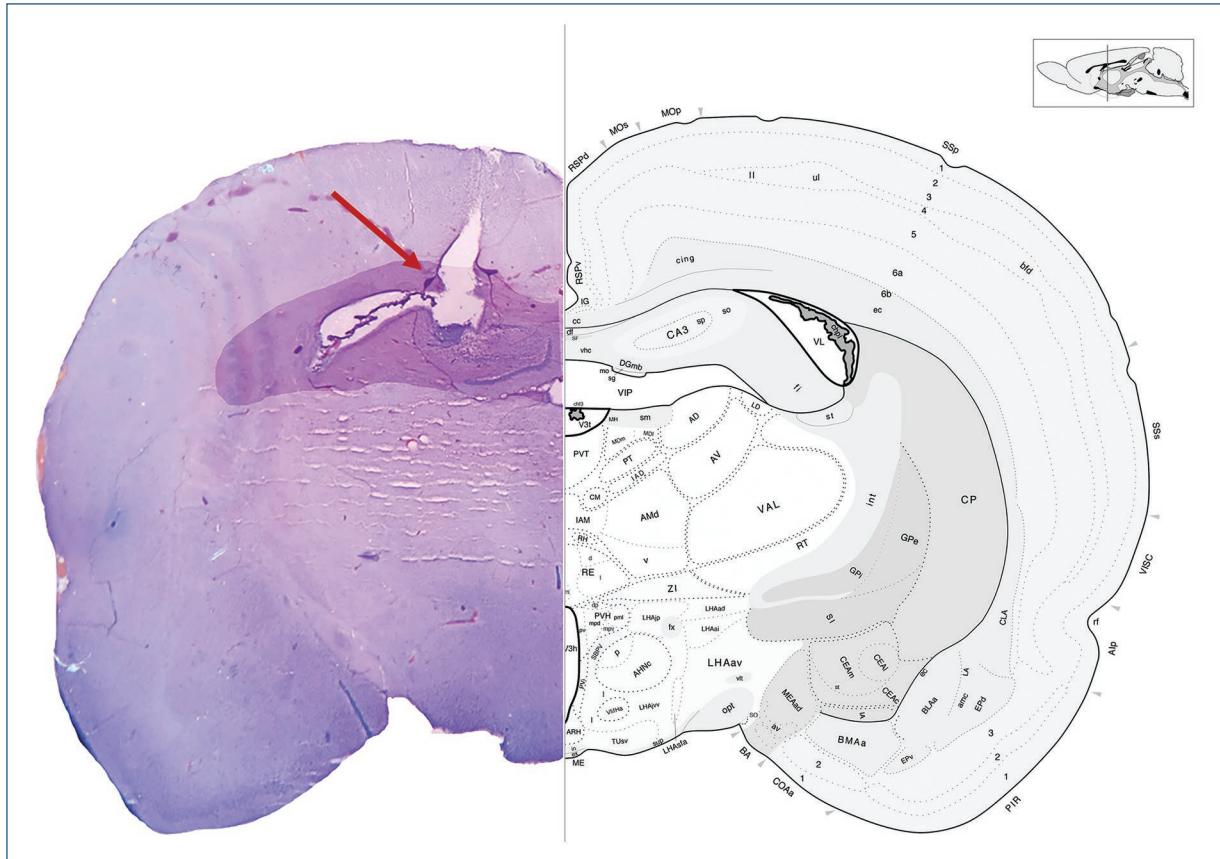


Figure 2. Photomicrograph presentative for the infusion site in dorsal hippocampus. The arrow indicates the site of the injection.

positions were corroborated by microscopy (Fig. 2) and compared with the described by²⁵.

Experimental limitations

As the nature of this study is preliminary, there are some limitations that authors want to admit: (i) high i.c.v. volumes (i.e., 1 μ L) were injected due to the solubility limitations of compounds; (ii) DMSO 10% was necessary as a dissolvent of compounds; and (iii) a single dose of drugs was used. Thus, no dose-dependence behavior was analyzed.

Statistical analysis

Data were analyzed using Sigma Plot 12.0 software (Systat Software Inc., San Jose, CA, USA). A t-paired test was performed for each of the quantitative variables for CPP-paradigm. Blinding of operators was not possible as the counter-balanced scheme complicated it. However, data analysis was performed in a blind design by different authors from those who conducted

the experiments. For all tests, the measure of central tendency was the mean, while the measure of dispersion was the standard error of the mean. Statistical significance was considered at $p < 0.05$.

Results

Figure 3A shows that intradorsal hippocampus injections of the vehicle (DMSO 10%) did not produce change ($t_3 = 0.268$, $p > 0.05$) in the time spent in the saline paired chamber in the test day compared versus baseline. Moreover, nicotine (0.6 mg/kg, s.c.) increased the time spent in the paired chamber after the conditioning phase compared with baseline ($t_5 = -2.626$, $p < 0.05$) in intact rats (Fig. 3B).

Subjects that received an intradorsal hippocampus pre-treatment with vehicle (DMSO 10%) during the conditioning phase increased their preference for the nicotine-paired chamber compared with the baseline ($t_7 = -2.898$, $p < 0.05$; Fig. 3C). In contrast, both ML-184 (0.48 nmol; a GPR55 agonist) and CID1602046 (1.16 nmol; a GPR55 antagonist) prevented

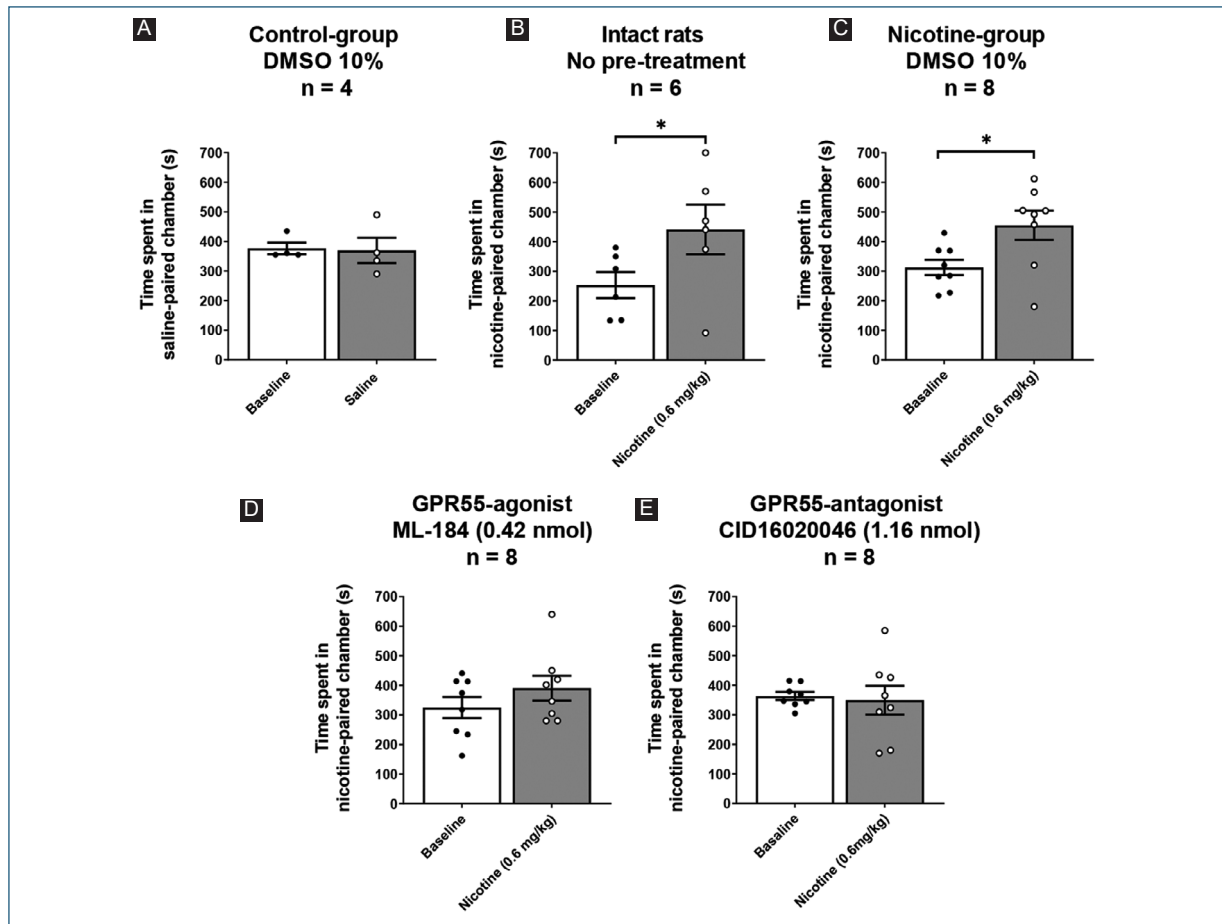


Figure 3. Effect of intradorsal-hippocampus injections of dimethyl sulfoxide (DMSO) 10% $n = 4$; **A:** on the time spent in the saline-paired chamber (1 mL/kg) or no-pretreatment intact rats; $n = 6$; **B:** vehicle DMSO 10%; $n = 8$; **C:** ML-184 (0.42 nmol; $n = 8$; **D:** or CID16020046 1.16 nmol; $n = 8$; **E:** on the nicotine-induced CPP (0.03 mg/kg, s.c.), * $p < 0.05$ versus the corresponding baseline. Data are expressed as the mean \pm standard error of the mean and analyzed by t-paired.

the change in place preference induced by nicotine as the time spent during the baseline did not differ compared with the test condition ($t_7 = -1.106$, $p > 0.05$ and $t_7 = 0.387$, $p > 0.05$, respectively; **Figs. 3D** and **E**).

Discussion

Liu et al.²³ reported that: (i) systemic injection of a GPR55 agonist (i.e., O-1602) prevented nicotine-mediated CPP; (ii) 0.5 mg/kg of nicotine increased dopamine levels in serum (effect that was prevented by O-1602), but not in the nucleus accumbens (NAcc); and (iii) the selective knockdown of GPR55 in NAcc did not modified the preventive effects of O-1602 on nicotine-mediated CPP. Suggesting that other brain areas may be involved in the preventive actions of GPR55 against nicotine-induced CPP. We have previously shown that several GPR55-related drugs (i.c.v.) prevented nicotine-mediated CPP in rats²¹. The main

finding of the present study is the possible participation of the dorsal hippocampus as a site of action for GPR55-target drugs in the prevention of nicotine-induced CPP.

As GPR55 is functionally expressed in the rat's hippocampus, where it seems to have a role in spatial learning and memory¹⁹, it is possible that its basal activity was necessary for the correct functionality of the hippocampal connectome. To support the above notion, both stimulation and blockade of dorsal-hippocampal GPR55 have been reported to decrease place memory in rats¹⁹. Neuroanatomically, the dorsal hippocampus seems to modify the acquisition of contextual memories in cocaine-exposed rodents by impairing retrieval of place preference and extinction of place preference in the CPP paradigm after pharmacological stimulation of dorsal hippocampal GABA_A receptor². Likewise, the contextual reward behavior is related to the strength of synapses between the hippocampus and NAcc²⁷.

The reinforcement is directly related to the mesolimbic dopamine activity primordially on the ventral tegmental area and NAcc, in which hippocampal GPR55 seems to participate in increasing mesolimbic dopaminergic neuron fires²⁸. Hence, the hippocampal GPR55 seems to be a pharmacological target that may modulate the reinforcing actions of nicotine in the CPP paradigm.

It is non-sensical that an agonist and an antagonist at the same receptor (i.e., GPR55) exert the same functional outcome. However, this contradictory pharmacological behavior has also been reported in the striatum by an independent group²², which proposed that GPR55 could control a pivotal mechanism whose alteration in any direction interrupts the correct process. Clearly, this possibility is only speculative. Another more reasonable (but also speculative) explanation is that multiple receptors/mechanisms are involved. Admittedly, a limitation of our preliminary results is the lack of a dose-response curve that analyses several concentrations of different agonists and antagonists of GPR55.

Finally, it is important to highlight that GPR55 is a receptor involved in many central and peripheral physiologic and pathophysiologic conditions, including blood flow regulation, proliferation/cancer conditions, metabolic processes, and pain^{15-21,29-33}. Thus, any potential clinical application in which GPR55 may be involved must be extremely cautious.

Conclusion

Our findings suggest: (i) dorsal hippocampus may be involved in nicotine-induced CPP, and (ii) dorsal-hippocampal GPR55 may pharmacologically modulate (by preventing) the nicotine-induced CPP.

Author's contributions

B. A. Marichal-Cancino created the original idea and the experimental protocols. O. A. Colis-Arenas, A. Muñoz-Pelayo, and J. Chávez-Reyes performed the experiments and compiled the database. B. A. Marichal-Cancino and C. H. López-Lariz analyzed data, created the graphs, and wrote the manuscript. O. A. Colis-Arenas, A. Muñoz-Pelayo and J. Chávez-Reyes review and correct the manuscript. All authors agreed with the final version of the manuscript.

Funding

This investigation was supported by the Dirección General de Investigación y Posgrado from the

Autonomous University of Aguascalientes (Grant: PIFF24-1).

Conflicts of interest

The authors declare no conflicts of interest.

Ethical considerations

Protection of humans and animals. The authors declare that the procedures followed complied with the ethical standards of the responsible Human Experimentation Committee and adhered to the World Medical Association and the Declaration of Helsinki. The procedures were approved by the Institutional Ethics Committee.

Confidentiality, informed consent, and ethical approval. The study does not involve patient personal data nor requires ethical approval. The SAGER guidelines do not apply.

Declaration on the use of artificial intelligence. The authors declare that no generative artificial intelligence was used in the writing of this manuscript.

References

- Hoffman DC. The use of place conditioning in studying the neuropharmacology of drug reinforcement. *Brain Res Bull.* 1989;23:373-87.
- Hitchcock LN, Lattal KM. Involvement of the dorsal hippocampus in expression and extinction of cocaine-induced conditioned place preference. *Hippocampus.* 2018;28:226-38.
- Raybuck JD, Lattal KM. Differential effects of dorsal hippocampal inactivation on expression of recent and remote drug and fear memory. *Neurosci Lett.* 2014;569:1-5.
- Jia W, Kawahata I, Cheng A, Sasaki T, Sasaoka T, Fukunaga K. Amelioration of nicotine-induced conditioned place preference behaviors in mice by an FABP3 inhibitor. *Int J Mol Sci.* 2023;24:6644.
- Amirteymori H, Veisi A, Khaleghzadeh-Ahangar H, Mozafari R, Haghparast A. Involvement of orexin-2 receptors in the CA1 region of the hippocampus in the extinction and reinstatement of methamphetamine-induced conditioned place preference in the rats. *Peptides.* 2023;160:170926.
- Jamali S, Dezfouli MP, Kalbasi A, Daliri MR, Haghparast A. Selective modulation of hippocampal theta oscillations in response to morphine versus natural reward. *Brain Sci.* 2023;13:322.
- Helbing C, Brocka M, Scherf T, Lippert MT, Angenstein F. The role of the mesolimbic dopamine system in the formation of blood-oxygen-level dependent responses in the medial prefrontal/anterior cingulate cortex during high-frequency stimulation of the rat perforant pathway. *J Cereb Blood Flow Metab.* 2016;36:2177-93.
- De Jong JW, Vanderschuren LJ, Adan RA. The mesolimbic system and eating addiction: what sugar does and does not do. *Curr Opin Behav Sci.* 2016;9:118-25.
- Salamone John D, Correa M. The mysterious motivational functions of mesolimbic dopamine. *Neuron.* 2012;76:470-85.
- Kibret BG, Canseco-Alba A, Onaivi ES, Engidawork E. Crosstalk between the endocannabinoid and mid-brain dopaminergic systems: implication in dopamine dysregulation. *Front Behav Neurosci.* 2023;17:1137957.
- Vargas LS, Ramires Lima K, Piaia Ramborger B, Roehrs R, Izquierdo I, Mello-Carpes PB. Catecholaminergic hippocampal activation is necessary for object recognition memory persistence induced by one-single physical exercise session. *Behav Brain Res.* 2020;379:112356.
- Pu L, Bao GB, Xu NJ, Ma L, Pei G. Hippocampal long-term potentiation is reduced by chronic opiate treatment and can be restored by re-exposure to opiates. *J Neurosci.* 2002;22:1914-21.

13. Robledo-Menendez A, Vella M, Grandes P, Soria-Gomez E. Cannabinoid control of hippocampal functions: the where matters. *FEBS J.* 2022;289:2162-75.
14. Akimov MG, Gamisonia AM, Dudina PV, Gretskaia NM, Gaydaryova AA, Kuznetsov AS, et al. GPR55 receptor activation by the N-Acyl dopamine family lipids induces apoptosis in cancer cells via the nitric oxide synthase (nNOS) over-stimulation. *Int J Mol Sci.* 2021;22:622.
15. Calvillo-Robledo A, Cervantes-Villagrana RD, Morales P, Marichal-Cancino BA. The oncogenic lysophosphatidylinositol (LPI)/GPR55 signaling. *Life Sci.* 2022;301:120596.
16. Morales P, Guerrero-Alba R, Marichal-Cancino BA. Linking the G-protein-coupled receptor 55 (GPR55) to the cannabinoid receptors (CB1 and CB2): a new narrative. In: Martin CR, Patel VB, Preedy VR, editors. *Cannabis Use, Neurobiology, Psychology, and Treatment.* Ch. 29. Cambridge: Academic Press; 2023. p. 395-406.
17. Marichal-Cancino BA, Sanchez-Fuentes A, Mendez-Diaz M, Ruiz-Contreras AE, Prospero-Garcia O. Blockade of GPR55 in the dorsolateral striatum impairs performance of rats in a T-maze paradigm. *Behav Pharmacol.* 2016;27:393-6.
18. Marichal-Cancino BA, Fajardo-Valdez A, Ruiz-Contreras AE, Mendez-Diaz M, Prospero-Garcia O. Advances in the physiology of GPR55 in the central nervous system. *Curr Neuropharmacol.* 2017;15:771-8.
19. Marichal-Cancino BA, Fajardo-Valdez A, Ruiz-Contreras AE, Mendez-Diaz M, Prospero-Garcia O. Possible role of hippocampal GPR55 in spatial learning and memory in rats. *Acta Neurobiol Exp (Wars).* 2018;78:41-50.
20. Vázquez-León P, Miranda-Páez A, Calvillo-Robledo A, Marichal-Cancino BA. Blockade of GPR55 in dorsal periaqueductal gray produces anxiety-like behaviors and evokes defensive aggressive responses in alcohol-pre-exposed rats. *Neurosci Lett.* 2021;764:136218.
21. Díaz-Barba A, Calvillo-Robledo A, Vázquez-León P, Gallegos-Vieyra E, Quintanar JL, Marichal-Cancino BA. Central GPR55 may prevent nicotine reinforcing actions: a preliminary study. *Acta Neurobiol Exp (Wars).* 2022;82:304-14.
22. Fatemi I, Abdollahi A, Shamsizadeh A, Allahtavakoli M, Roohbakhsh A. The effect of intra-striatal administration of GPR55 agonist (LPI) and antagonist (ML193) on sensorimotor and motor functions in a parkinson's disease rat model. *Acta Neuropsychiatr.* 2021;33:15-21.
23. Liu Q, Yu J, Li X, Guo Y, Sun T, Luo L, et al. Cannabinoid receptor GPR55 activation blocks nicotine use disorder by regulation of AMPAR phosphorylation. *Psychopharmacology (Berl).* 2021;238:3335-46.
24. Bayne K. Revised guide for the care and use of laboratory animals available. *American Physiological Society. Physiologist.* 1996;39:199, 208-11.
25. Paxinos G, Watson C. *The Rat Brain in Stereotaxic Coordinates.* 7th ed. New York: Academic Press; 2014.
26. Calvillo-Robledo A, Samson-Soleil, Marichal-Cancino BA, Medina-Pizaño MY, Ibarra-Martínez D, Ventura-Juárez J, et al. Rapid liver self-recovery: a challenge for rat models of tissue damage. *Life Sci.* 2024;357:122975.
27. LeGates TA, Kvarita MD, Tooley JR, Francis TC, Lobo MK, Creed MC, et al. Reward behaviour is regulated by the strength of hippocampus-nucleus accumbens synapses. *Nature.* 2018;564:258-62.
28. Kramar C, Loureiro M, Renard J, Laviolette SR. Palmitoylethanolamide modulates GPR55 receptor signaling in the ventral hippocampus to regulate mesolimbic dopamine activity, social interaction, and memory processing. *Cannabis Cannabinoid Res.* 2017;2:8-20.
29. Guerrero-Alba R, Barragan-Iglesias P, Gonzalez-Hernandez A, Valdez-Morales EE, Granados-Soto V, Condes-Lara M, et al. Some prospective alternatives for treating pain: the endocannabinoid system and its putative receptors GPR18 and GPR55. *Front Pharmacol.* 2018;9:1496.
30. Marichal-Cancino BA, Altamirano-Espinoza AH, Manrique-Maldonado G, MaassenVanDenBrink A, Villalón CM. Role of pre-junctional CB1, but not CB2, TRPV1 or GPR55 receptors in anandamide-induced inhibition of the vasodepressor sensory CGRpergic outflow in pithed rats. *Basic Clin Pharmacol Toxicol.* 2014;114:240-7.
31. Marichal-Cancino BA, González-Hernández A, MaassenVanDenBrink A, Ramírez-San Juan E, Villalón CM. Potential mechanisms involved in palmitoylethanolamide-induced vasodepressor effects in rats. *J Vasc Res.* 2020;57:152-63.
32. Marichal-Cancino BA, Manrique-Maldonado G, Altamirano-Espinoza AH, Ruiz-Salinas I, Gonzalez-Hernandez A, Maassenvandenbrink A, et al. Analysis of anandamide- and lysophosphatidylinositol-induced inhibition of the vasopressor responses produced by sympathetic stimulation or noradrenaline in pithed rats. *Eur J Pharmacol.* 2013;721:168-77.
33. Ramirez-Orozco RE, Garcia-Ruiz R, Morales P, Villalón CM, Villafan-Bernal JR, Marichal-Cancino BA. Potential metabolic and behavioural roles of the putative endocannabinoid receptors GPR18, GPR55 and GPR119 in feeding. *Curr Neuropharmacol.* 2019;17:947-60.

Idiopathic hypertrophic spinal pachymeningitis: a diagnostic challenge. Case report

Paquimeningitis espinal hipertrófica idiopática: un desafío diagnóstico. Reporte de caso

César A. Almendárez-Sánchez, Carlos Morales-Valencia*^{ORCID}, Leonardo Álvarez-Vázquez, Arturo de J. Gómez-Cano, and Antonio Sosa-Nájera

Department of Neurosurgery, Centro Médico Licenciado Adolfo López Mateos, Instituto de Salud del Estado de México, Toluca, State of Mexico, Mexico

Abstract

Hypertrophic spinal pachymeningitis is an unusual disease. It may be idiopathic or secondary to other diseases. The main characteristics are chronic inflammation and hypertrophy of the spinal dura mater, with resulting neurological deficits such as sensory and motor alterations. Treatment by surgical decompression combined with systemic steroids has a positive impact. The objective is to report a clinical case of hypertrophic spinal pachymeningitis since it is an extremely rare and little-known entity. A 65-year-old female patient, whose condition began on August 1, 2022, with stabbing pain in the dorsal region, without irradiation, without predominance of time. Three months after the onset of his current condition, there was a decrease in strength in bilateral pelvic limbs 3/5, as well as hypoesthesia in the pelvic limbs. Contrast-enhanced magnetic resonance imaging of the spine is requested; all sequences are reviewed where the contrast-enhanced T1 sequence highlights a lesion that generates narrowing at the level of the thoracic spine with an increase in volume and enhancement of contrast medium from T2 to T10 in the anterior and posterior spinal region. A biopsy of the lesion was obtained, which in the pathology report was concluded as hypertrophic spinal pachymeningitis and treatment with steroids was started immediately. Hypertrophic spinal pachymeningitis is an extremely rare entity, and there is scarce information published in the literature about it. Therefore, making a timely diagnosis to select the most appropriate treatment for patients is important.

Keywords: Hypertrophic spinal pachymeningitis. Spinal cord. Meningioma. Upper motor neuron.

Resumen

La paquimeningitis espinal hipertrófica es una enfermedad rara. Puede ser idiopática o secundaria a otras enfermedades. La característica principal es la inflamación crónica e hipertrofia de la duramadre espinal con déficits neurológicos resultantes como alteraciones a nivel sensitivo y motor. El tratamiento mediante descompresión quirúrgica aunado a esteroides sistémicos tiene un impacto positivo. El objetivo es reportar un caso clínico de paquimeningitis espinal hipertrófica, ya que es una entidad extremadamente rara y poco conocida. Paciente de sexo femenino de 65 años, que inicia su padecimiento el 1 de agosto del 2022, con dolor en región dorsal de tipo punzante, sin irradiaciones, sin predominio de horario. Tres meses posteriores al inicio de su padecimiento actual se agrega disminución de la fuerza en miembro pélvicos bilaterales 3/5, así como hipoestesia en miembros pélvicos. Se solicita resonancia magnética contrastada de columna, se revisan todas las secuencias en donde resalta en secuencia T1 contrastada lesión que genera estrechamiento a nivel de columna torácica

*Correspondence:

Carlos Morales-Valencia
E-mail: carlosmorales175@hotmail.com

Date of reception: 12-11-2024
Date of acceptance: 13-11-2024
DOI: 10.24875/ANCE.M24000043

Available online: 24-04-2025
Arch Neurocién (Eng). 2025;30(4):180-183
www.archivosdeneurociencias.mx

3081-1562 / © 2024 Instituto Nacional de Neurología y Neurocirugía. Published by Permanyer. This is an open access article under the CC BY-NC-ND license (<http://creativecommons.org/licenses/by-nc-nd/4.0/>).

con aumento de volumen y refuerzo al medio de contraste desde T2 hasta T10 en región medular anterior y posterior. Se obtiene biopsia de la lesión, la cual en reporte de patología se concluye como paquimeningitis espinal hipertrófica, y se inicia de forma inmediata tratamiento con esteroides. La paquimeningitis espinal hipertrófica es una entidad extremadamente rara, en la que existe poca información publicada en la literatura. Por lo que es de importancia realizar el diagnóstico oportuno para seleccionar el tratamiento más adecuado para los pacientes.

Palabras clave: Paquimeningitis espinal hipertrófica. Médula espinal. Meningioma. Neurona motora superior.

Introduction

Spinal hypertrophic pachymeningitis is a rare inflammatory disorder characterized by chronic diffuse fibrosis and thickening of the dura mater¹. It is a diagnosis of exclusion, requiring the exploration of various pathological entities as potential causes of symptoms², including sarcoidosis³, rheumatoid arthritis⁴, granulomatosis with polyangiitis (Wegener's)⁵, metabolic diseases⁶, tuberculosis, fungal meningitis, and meningococcal meningitis. Therefore, a thorough investigation is necessary to confirm the idiopathic etiology of the disease process⁷. Spinal hypertrophic pachymeningitis can occur anywhere along the craniospinal axis, from the brain to the spinal cord. The spinal form clinically presents with weakness, ataxia, and sensory loss due to compression of surrounding structures and is one of the rare causes of radiculomyelopathy. Most cases of spinal hypertrophic pachymeningitis require surgical decompression to prevent complications and neurological relapses⁸.

Case report

A female patient in her 7th decade of life, with no significant past medical history, began experiencing symptoms on August 1st, 2022, with burning pain in the dorsal region, without a specific time predominance. Three months after the initial symptoms, she developed bilateral lower limb weakness. On physical examination, the patient had a Glasgow Coma Scale score of 15, with 2 mm isocoric and normoreactive pupils, and intact higher mental functions. Motor examination revealed normotonia and normotrophy, with muscle strength in the upper limbs (C4, C5, C6, C7, C8, T1) rated 5/5 bilaterally on the Daniels scale. In the lower limbs (L1, L2, L3, L4, L5, S1), strength was 3/5 bilaterally. Reflexes included bilateral biceps, triceps, and brachioradialis ++/++++, and patellar and Achilles reflexes +++/++++. Plantar responses were extensor bilaterally. Exteroceptive and proprioceptive sensitivity were compromised at the T5 level. There was no loss of sphincter control. The patient remained afebrile during her hospital stay. Lab test results showed no

leukocytosis (white blood cell count: 6.7 cells/mm³). The erythrocyte sedimentation rate (ESR) was elevated at 49 mm/h, and C-reactive protein (CRP) levels were also elevated at 38 mg/L. Serological tests for HIV and VDRL tested negative. Rheumatoid factor was 25 IU/mL (normal: < 20 IU/mL), IgG was 3,650 mg/dL (normal: 700-1600 mg/dl), IgA was 887 mg/dL (normal: 70-400 mg/dl), and IgM was 75 mg/dL (normal: 40-230 mg/dl). Anti-SS-A antibodies and antinuclear antibodies were not elevated. Liver and kidney function tests were normal. A total spine MRI with contrast was performed. On T1-weighted contrast-enhanced images, a lesion was observed at thoracic spine level, with increased volume and contrast enhancement from T2 to T10 in the anterior and posterior spinal regions. Axial views showed marked extrinsic spinal cord compression at T5-T6, raising suspicion of a spinal meningioma (Fig. 1). Surgical treatment was decided upon, involving a posterior thoracic approach, posterior arthrodesis T4-T7 with transpedicular screws, laminectomy T5-T6, durotomy, biopsy, and duraplasty, with placement of lateral rods and crosslink. The biopsy specimen was sent for pathology, which reported idiopathic spinal hypertrophic pachymeningitis (Fig. 2). Steroid treatment was initiated. Upon discharge, the patient was referred to physical therapy and rehabilitation. She was followed up in outpatient clinics for 11 months, showing improvement in lower limb strength (5/5 on the Daniels scale) without additional neurological deficits.

Discussion

This disease can involve intracranial and spinal regions. The spinal form is extremely rare and may be associated with myelopathy, radiculopathy, or both. It is included in the spectrum of IgG4-related diseases, characterized by diffuse fibrosis along with lymphoplasmacytic infiltration rich in tissue plasma cells positive for IgG4⁹. Diagnosing spinal hypertrophic pachymeningitis is challenging even with imaging modalities like MRI, and most cases require histopathological confirmation¹⁰.

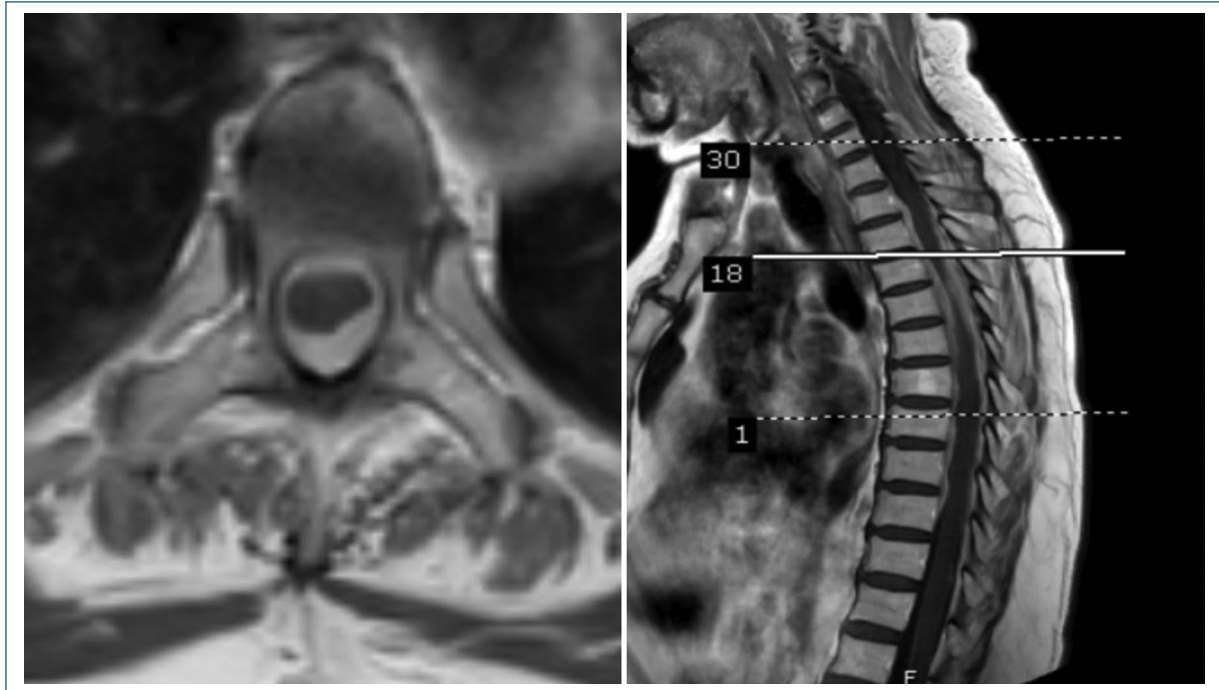


Figure 1. Axial T1-weighted MRI at T5-T6 showing an intradural extramedullary lesion causing spinal cord compression (left) and sagittal view (right) showing increased volume and contrast enhancement from T2 to T10 in the anterior and posterior spinal regions.

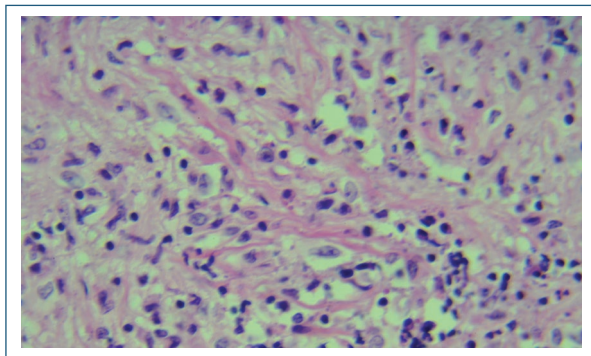


Figure 2. Histopathological examination of the dural mass showed extensive fibrosis with lymphoplasmacytic infiltration on hematoxylin and eosin staining.

Signs and symptoms of spinal hypertrophic pachymeningitis develop gradually, from nerve root compression to spinal cord compression, with nearly all patients experiencing progressive paraparesis^{11,12}.

MRI is the most useful diagnostic modality for idiopathic spinal hypertrophic pachymeningitis^{13,14}. The lesion is typically hypointense on T2-weighted images and shows contrast enhancement on T1-weighted images. However, differentiating idiopathic spinal hypertrophic pachymeningitis from an epidural abscess or

spinal tumor is difficult based solely on imaging without dural biopsy or surgical removal¹⁴.

The gold standard diagnostic test for these cases is an open biopsy of the thickened dura mater. However, biopsies often reveal nonspecific inflammatory changes, including plasma cells, giant cells, neutrophils, eosinophils, and lymphocytes^{15,16}.

Surgical decompression is recommended to relieve symptoms and neurological sequelae with definitive spinal cord decompression^{17,18}. Most cases of idiopathic spinal hypertrophic pachymeningitis show significant improvement and reduced relapse susceptibility when combining surgical decompression with postoperative pulse steroids. Postoperative corticosteroid therapy is also effective in controlling residual hypertrophic lesions, particularly when located in the ventral space¹⁹. Some studies have proposed other treatment options, such as radiotherapy, methotrexate, cyclophosphamide, empirical therapy, or antituberculosis treatment. However, the efficacy of such therapies remains unclear²⁰.

Conclusions

Spinal hypertrophic pachymeningitis is a rare cause of dural thickening that shows chronic progressive

neurological symptoms. On MRI, findings of an extramedullary mass extending over multiple vertebral levels, strongly hypointense signal on T2-weighted sequences, and intense peripheral enhancement are suggestive of the diagnosis. Differential diagnostic considerations include epidural hematoma, epidural abscess, spinal tumor, and ossification of the posterior longitudinal ligament.

Authors' contributions

C.A. Almendárez-Sánchez: drafting, reviewing, editing. C. Morales-Valencia: drafting, reviewing, editing. L. Álvarez-Vázquez: drafting, reviewing, editing. A.J. Gómez-Cano: reviewing, editing. A. Sosa-Nájera: reviewing, editing.

Funding

This research has not received any specific grants from public, commercial, or for-profit agencies.

Conflicts of interest

The authors declare no conflicts of interest.

Ethical considerations

Protection of human and animal subjects. The authors declare that no experiments were performed on humans or animals for this research.

Confidentiality, informed consent, and ethical approval. The authors followed their institution's confidentiality protocols, obtained informed consent from patients, and received approval from the Ethics Committee. The SAGER guidelines were followed according to the nature of the study.

Declaration on the use of artificial intelligence.

The authors declare that no generative artificial intelligence was used in the writing of this manuscript.

References

- Gupta A, Um D, Samant R. Idiopathic hypertrophic spinal pachymeningitis. *J Med Cases*. 2023;14(12):405-12.
- Slade SJ, Bauer EM, Stone VV, Dave AJ. Spinal IgG4-related hypertrophic pachymeningitis with spinal cord compression case report. *World Neurosurg*. 2019;130:65-70.
- Huang H, Haq N. Spinal leptomeningeal sarcoidosis. 1987;29(1):100.
- Gutmann L, Hable K. Rheumatoid pachymeningitis. *Neurology*. 1963;13:901-5.
- Nishino H, Rubino FA, Parisi JE. The spectrum of neurologic involvement in Wegener's granulomatosis. *Neurology*. 1993;43(7):1334-7.
- Paulson GW, Meagher JN, Burkhardt J. Spinal pachymeningitis secondary to mucopolysaccharidosis. Case report. *J Neurosurg*. 1974;41(5):618-21.
- Uemura K, Matsumura A, Kobayashi E. Idiopathic chronic hypertrophic craniocervical pachymeningitis: case report. *Neurosurgery*. 1995;37(2):358.
- Alsulaiman A. Idiopathic hypertrophic spinal pachymeningitis: a diagnostic challenge: a case report and review of the literature. *J Neurosci Rural Pract*. 2020;11(1):175-7.
- Araújo Melo LL, Daher MT, Gonçalves MVM, Freitas MB. Idiopathic hypertrophic spinal pachymeningitis: a case report. *Rev Bras Ortop (Sao Paulo)*. 2021;57(3):521-3.
- Mikawa Y, Watanabe R, Hino Y. Hypertrophic spinal pachymeningitis. *Spine (Phila Pa 1976)*. 1994;19(5):620-5.
- Bucy PC, Freeman LW. Hypertrophic spinal pachymeningitis with special reference to appropriate surgical treatment. *J Neurosurg*. 1952;9(6):564-78.
- Guidetti B, La Torre E. Hypertrophic spinal pachymeningitis. *J Neurosurg*. 1967;26(5):496-503.
- Ashkenazi E, Constantini S, Pappo O, Gomori M, Averbuch-Heller L, Umansky F. Hypertrophic spinal pachymeningitis: report of two cases and review of the literature. *Neurosurgery*. 1991;28(5):730-2.
- Pai S, Welsh CT, Patel S, Rumboldt Z. Idiopathic hypertrophic spinal pachymeningitis: report of two cases with typical MR imaging findings. *AJNR Am J Neuroradiol*. 2007;28(3):590-2.
- Hamilton SR, Smith CH, Lessell S. Idiopathic hypertrophic cranial pachymeningitis. *J Clin Neuroophthalmol*. 1993;13(2):127-34.
- Ranasinghe MG, Zalatimo O, Rizk E, Specht CS, Reiter GT, Harbaugh RE, et al. Idiopathic hypertrophic spinal pachymeningitis. *J Neurosurg Spine*. 2011;15(2):195-201.
- Botella C, Orozco M, Navarro J, Riesgo P. Idiopathic chronic hypertrophic craniocervical pachymeningitis: case report. *Neurosurgery*. 1994;35(6):1144-9.
- Ito Z, Osawa Y, Matsuyama Y, Aoki T, Harada A, Ishiguro N. Recurrence of hypertrophic spinal pachymeningitis. Report of two cases and review of the literature. *J Neurosurg Spine*. 2006;4(6):509-13.
- Tosa M, Hara M, Morita A, Ninomiya S, Ebashi M, Kamei S, et al. Idiopathic hypertrophic spinal pachymeningitis. *Intern Med*. 2015;54(15):1923-6.
- Qin LX, Wang CY, Hu ZP, Zeng LW, Tan LM, Zhang HN. Idiopathic hypertrophic spinal pachymeningitis: a case report and review of literature. *Eur Spine J*. 2015;24(Suppl 4):S636-43.

Removal of non-tumorous ovaries in anti-NMDAR receptor encephalitis. Report of 2 cases and literature review

Extirpación de ovarios no tumorales en encefalitis anti-NMDAR. Informe de dos casos y revisión bibliográfica

Ana L. Calderón-Garcidueñas*^{ORCID} and Diego I. Talavera-Bazán^{ORCID}

Department of Neuropathology, Instituto Nacional de Neurología y Neurocirugía Manuel Velasco Suárez, Mexico City, Mexico

Abstract

Anti-N-methyl-D-aspartate receptor (NMDAR) encephalitis is a form of autoimmune limbic encephalitis mediated by antibodies against the GluN1 (or NR1) subunit of the NMDAR. It is associated up to 56% with the presence of teratomas. Based on two cases, we analyze the literature that supports the use of oophorectomy when evidence of neoplasia by imaging is lacking.

Keywords: N-methyl-D-aspartate receptor encephalitis. Limbic encephalitis. Bilateral oophorectomy. Clinical evolution.

Resumen

La encefalitis anti-receptor NMDA (anti-NMDAR) es una forma de encefalitis límbica autoinmune mediada por anticuerpos contra la subunidad GluN1 (o NR1) del NMDAR y se asocia hasta en un 56% con la presencia de teratomas. A partir de dos casos, analizamos el respaldo de la literatura para realizar ooforectomía cuando no hay evidencia de neoplasia por imagen.

Palabras clave: Encefalitis anti-receptor NMDA. Encefalitis límbica. Ooforectomía bilateral. Evolución clínica.

*Correspondence:

Ana L. Calderón-Garcidueñas
E-mail: ana.calderon@innn.edu.mx

Date of reception: 06-11-2024
Date of acceptance: 25-03-2025
DOI: 10.24875/ANC.24000015

Available online: 18-07-2025
Arch Neurocién (Eng). 2025;30(4):184-190
www.archivosdeneurociencias.mx

3081-1562 / © 2025 Instituto Nacional de Neurología y Neurocirugía. Published by Permanyer. This is an open access article under the CC BY-NC-ND license (<http://creativecommons.org/licenses/by-nc-nd/4.0/>).

Introduction

Anti-N-methyl-D-aspartate receptor (NMDAR) encephalitis is an autoimmune condition that manifests through diverse and intricate neuropsychiatric symptoms. It primarily impacts young women and is frequently linked to the presence of an ovarian teratoma. Since its description in 2005, first clinically¹ and then associated with neuronal surface receptors, specifically glutamate NMDAR, NR1, and NR2², anti-NMDAR encephalitis has become the leading cause of autoantibody-mediated encephalitis in children, adolescents, and young adults³. It is usually characterized by cognitive impairment or psychiatric symptoms that progress rapidly in girls or young female patients who can also present abnormal movements, seizures, or coma. Anti-NMDAR encephalitis is a state of hypofunction⁴. The immunoglobulin G (IgG) antibodies are directed at the extracellular domain of the GluN1 subunit of the NMDAR located on the surface of neurons. The effect of this union is the internalization of NMDARs, resulting in a reversible functional reduction of NMDARs with hypofunction. The central NMDAR regulates glutamate-dependent excitatory synaptic transmission and synaptic plasticity⁴. GABAergic cortical interneurons are the primary target of antibodies targeting the GluN1 subunit; the inhibition of excitatory neurons decreases markedly, which may explain the psychosis symptom of anti-NMDAR encephalitis; decreased transport of excitatory neurotransmitters caused by NMDAR antibodies may be the cause of seizures in these patients. Ovarian teratomas and herpes simplex virus infections are the main causes of anti-NMDAR encephalitis⁴. Ovarian teratoma is a germ cell tumor containing tissues derived from all three germ layers. It may contain neuronal cells exposed to the immune system, triggering an antibody response that can attack normal brain neurons⁴.

It primarily affects young women and is often associated with an ovarian teratoma. It is a serious yet treatable condition if diagnosed early. Its treatment involves immunotherapy and surgical removal of the teratoma of the ovaries.

When cases of NMDAR-associated encephalitis in young women are reviewed, there are two scenarios: patients with or without neoplasia, generally an ovarian teratoma. Literature supports that teratoma resection leads to the disappearance of symptoms or at least to better control of them, with a better prognosis for patients⁵. However, bilateral oophorectomy in the absence of an identifiable neoplasm by imaging is controversial because it leaves a young woman without the possibility of having

biological children of her own. We present two cases of young women with this pathology in whom, in one of them, a teratoma was initially resected. Then, the contralateral ovary was removed, and in a second case, this procedure was performed without evidence of neoplasia. Based on two cases, we analyze the literature that supports the use of oophorectomy when evidence of neoplasia by imaging is lacking.

Presentation of the cases

Case 1

A 25-year-old woman, a university student, began insidiously in May 2016 with bitemporal headache,odynophagia, and fever; with a diagnosis of pharyngotonsillitis, she received amoxicillin/clavulanic acid and non-steroidal analgesics. In the following week, the headache progressed to being disabling; incongruous, repetitive speech, soliloquies, coprolalia, laughter for no external reason, agitation, and aggressiveness were added, which initially fluctuated. In June, she went to a local hospital where she had a generalized tonic-clonic seizure and psychomotor agitation. Ceftriaxone, vancomycin, acyclovir, and dexamethasone were prescribed. However, she persisted with oculogyric seizures, dystonic movements, and ballismus. Limbic encephalitis was suspected, and a left ovarian teratoma was detected and resected. Pre-surgical blood tumor marker values were normal except for CA125 antigen (23.4 U/mL; normal < 20 U/mL). Methylprednisolone was administered (1 g × 3 doses), followed by oral prednisone concomitantly with five plasmapheresis sessions and antiepileptic management. The patient presented episodes of paroxysmal hyperthermia of 42 °C, accompanied by dysautonomia. In August, she was referred to our hospital. Brain magnetic resonance image (MRI) showed diffuse cortical hyperintensity on T2 and fluid-attenuated inversion recovery (FLAIR) sequences; the electroencephalogram (EEG) showed severe generalized dysfunction. Anti-NMDA antibodies were positive in blood and cerebrospinal fluid (CSF). In the intense care unit (ICU), ventilatory support was provided, and the refractory status epilepticus was resolved, with persistence of temperature > 40°C, for which a therapeutic hypothermia suit was placed. Imaging studies showed the absence of the left ovary and the presence of a normal right ovary. She presented diabetes insipidus of central origin managed with desmopressin. On September 26th, she received her last dose of cyclophosphamide.

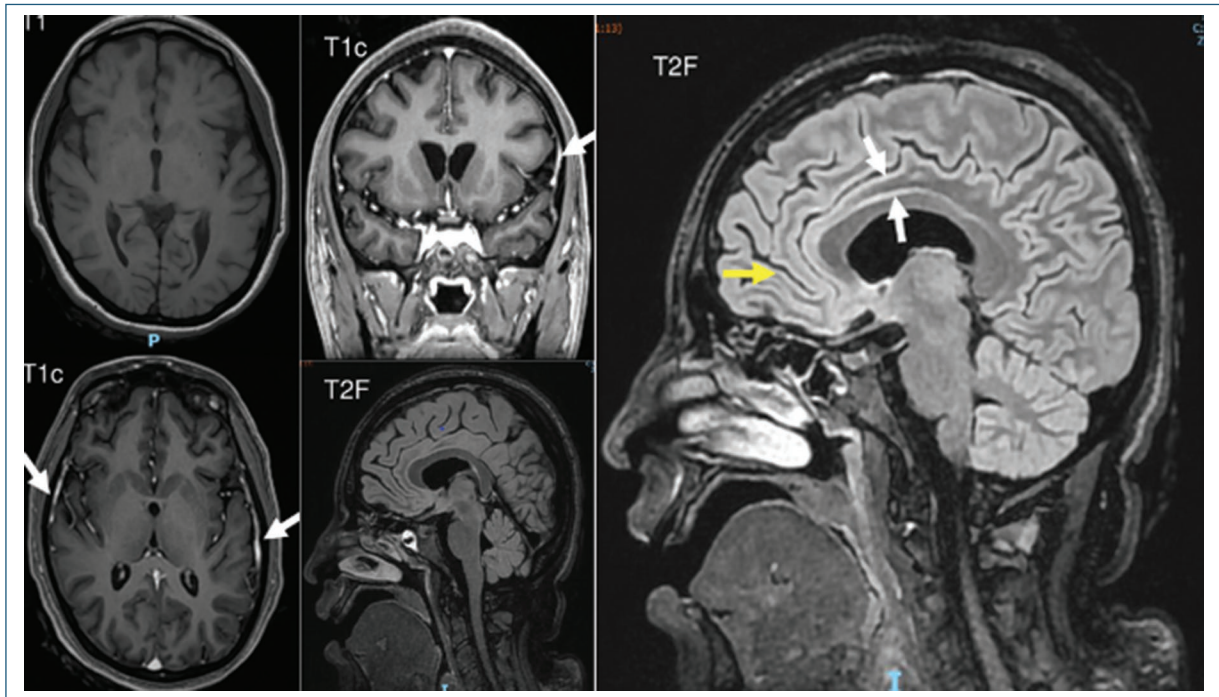


Figure 1. RMN. T1-weighted magnetic resonance image (MRI) showed a slight decrease in bilateral frontal cortical volume. T1c sequences showed areas of hyperintensity in coronal (top) and axial (bottom) sections of the leptomeninges; increased signal intensity was also observed in cortical gray matter in the frontomedial (yellow arrow) and bilateral anterior cingulate regions (white arrows).

Due to the persistence of symptoms, a laparoscopic oophorectomy was performed on October 4th; therapy with plasmapheresis was started and, on November 7, the seventh and last session of plasmapheresis was given, with clinical improvement in respiratory function; she had a patent percutaneous tracheostomy, and was tolerating oxygen delivery through a continuous nebulizer, for more than 72 h. The non-traumatic Glasgow score at that time was 10 points. She was seizure-free, presented spontaneous, inattentive eye-opening, minimal dyskinetic movements in both extremities, hemodynamically stable, without vasopressor requirement, with a systemic blood pressure of 120/60 mmHg, patent gastrostomy, normal abdomen, and mild, normocytic, normochromic anemia. Under these conditions, the patient was transferred to her assigned hospital to continue recovery.

Case 2

She was a 31-year-old woman with a PhD in Economics. The patient smoked in the past 13 years (12 cigarettes/day), was diagnosed with depression in 2020, and received treatment with sertraline until 2022.

She began on July 12, 2022, with short-term memory alteration, and a week later, two seizure episodes, 15 min apart; she was referred to our hospital with a diagnosis of encephalitic syndrome. At admission on July 19, she showed incongruent speech, ideas of aggression toward her pets, psychomotor agitation, and insomnia; she was inattentive, disoriented in time, place, and situation, with delusional ideas of harm, and positive right Hoffman and Tromner signs. She also had dysautonomias with a heart rate between 110 and 180/min. The CSF examination showed pleocytosis > 5 cells, positive oligoclonal bands, and anti-NMDA antibodies. Film-array and GeneXpert tests were negative. EEG showed four electrographic seizures of right frontal-temporal onset and interictal period with wakefulness. Treatment was started with midazolam, lacosamide, and methylprednisolone boluses. MRI showed a slight decrease in bilateral frontal cortical volume, hyperintensity in leptomeninges, and increased signal intensity in cortical gray matter in the frontomedial and bilateral anterior cingulate regions (Fig. 1).

Tomography showed follicular cysts and discrete enlargement of both ovaries (31 × 20 × 27 mm, right; 33 × 25 × 26 mm, left). Plasmapheresis was started on July 24, with a total of five sessions. The patient

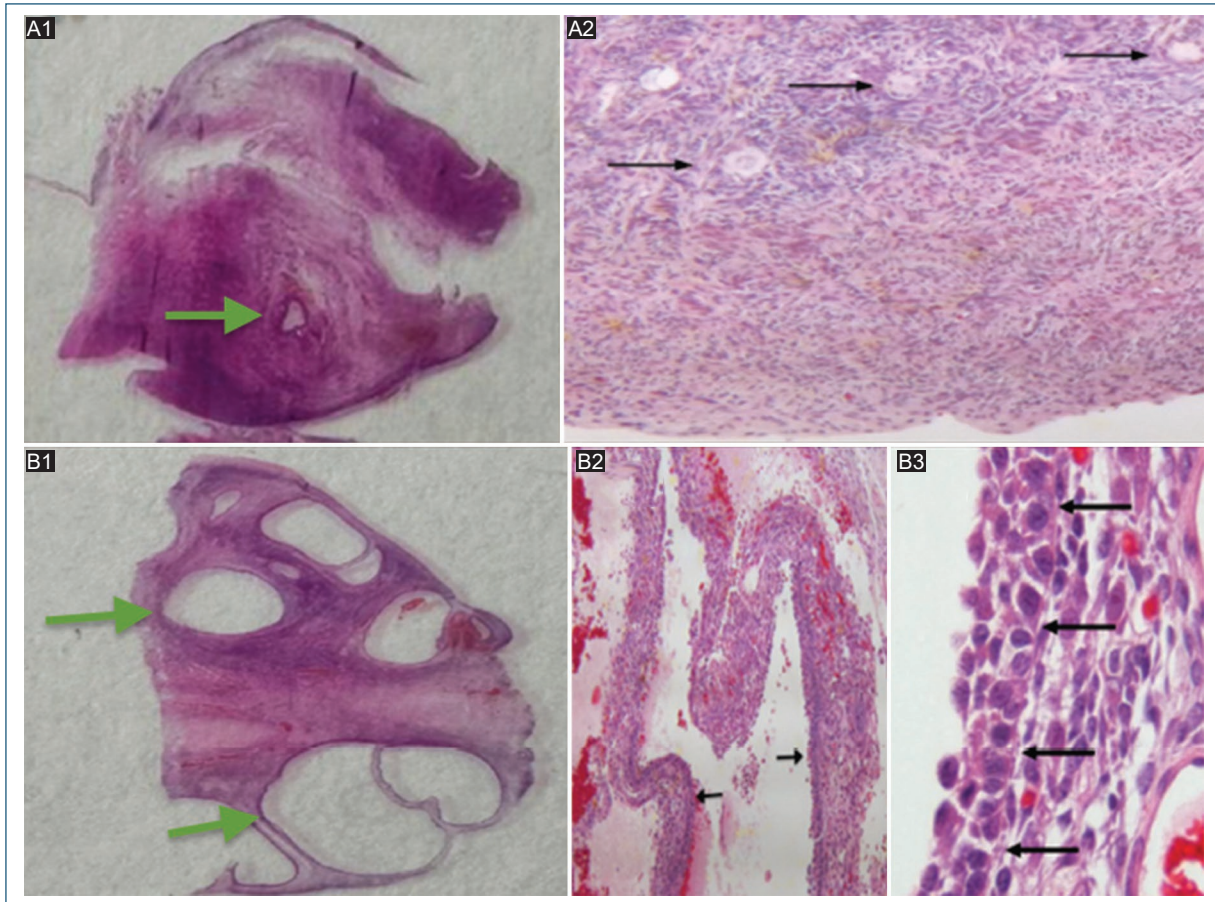


Figure 2. A: case 1. **A1:** histological montage of the ovary showing compact stroma with occasional simple cyst (arrow). **A2:** section of the ovary with normal primordial follicles (arrows). $\times 50$, H and E. **B:** case 2. **B1:** histological montage of the ovary showing different sizes of non-hemorrhagic cysts (arrows). **B2:** a follicular cysts (arrows). H and E $\times 100$. **B3:** follicular cysts are composed of an inner layer of granulosa cells (arrows) and an outer layer of theca cells. H and E $\times 400$.

presented a torpid evolution, with refractory status epilepticus, which was managed in the ICU from August 8 to 28. On August 10, a bilateral laparoscopic oophorectomy was performed. Later on, at the neurology service, hyperkinetic disorder with orolingual dyskinesias and facial spasms were observed. On September 5, she again presented an increase in the frequency of focal epileptic seizures (forced head deviation to the left and tonic posture in the right arm), and she remained under sedation until September 14, after the EEG corroborated the resolution. Finally, she presented clinical signs of distributive shock with non-infectious etiology identified, culture studies, and additional infectious biomarkers negative to infectious etiology. She presented uncontrolled dysautonomia, refractory to treatment, as well as hyperthermia. Finally, she developed respiratory distress, asystole, and death. Ovarian resection. Case 1.

Resection of right adnexa: the ovary was morphologically normal, with numerous primary follicles, corpus luteum in regression, some white bodies, and a simple cyst (2mm) (Fig. 2, A1-A2). Case 2. Bilateral ovary resection: ovaries showed normal primary follicles, follicular cysts, and theca granulosa cysts (Fig. 2, B1-B2). A chronic dilated salpingitis was observed.

Discussion

Anti-NMDAR encephalitis is a form of autoimmune limbic encephalitis mediated by antibodies against the GluN1 (or NR1) subunit of the NMDAR and is associated up to 56% with the presence of ovarian teratomas⁶.

One of our cases involved an ovarian teratoma, and both patients experienced a prolonged course of seizures, brain abnormalities on MRI, and dysautonomia.

In patients with anti-NMDAR encephalitis, between 10-50% experience autonomic dysfunction, which can lead to hemodynamic shock, increasing both morbidity and mortality⁷. Seizures occur in nearly 80% of patients during the acute phase, and around 50% show abnormal brain MRI findings⁸.

When a teratoma exists (2/3 of patients with anti-NMDAR encephalitis), it has been perfectly demonstrated that its resection contributes to clinical improvement, and the faster the resection is performed, the better the clinical response will be⁹. Suspecting the diagnosis of anti-NMDAR encephalitis is the first step to successful treatment; after a non-specific prodromal period that occurs in 40-70% of cases, behavioral and psychiatric manifestations occur in 90% of patients over 4 days to 2 weeks. A crucial part of the diagnosis is the neurological examination, which uses the warning signs to detect an autoimmune etiology, have an earlier diagnosis, and separate it from primary psychiatric disease.

In the study by Herkeb and Prüss aimed to identify patients with recent-onset psychosis who may have autoimmune encephalitis, yellow and red flags were mentioned. The first ones included rapid progression of psychosis (despite therapy), decreased levels of consciousness, catatonia, headache, aphasia or dysarthria, abnormal postures or movements (orofacial and limb dyskinesia), focal neurological deficits, autonomic instability, hyponatremia, and having other autoimmune diseases (e.g., thyroiditis). Red flags included epileptic seizures, faciobrachial dystonic seizures, suspected malignant neuroleptic syndrome, CSF lymphocytic pleocytosis or CSF-specific oligoclonal bands without evidence for infection, MRI abnormalities (mesiotemporal hyperintensities, atrophy pattern), and EEG abnormalities (slowing, epileptic activity or extreme delta brush)¹⁰.

Performing an EEG is essential to demonstrate abnormal electrical patterns and epileptogenic activity; CSF analysis is indispensable to rule out any infectious process and will show pleocytosis and oligoclonal bands. Search for a teratoma is mandatory. If available, searching IgG antibodies against the NR1 subunit of the NMDAR in CSF confirms the diagnosis⁹.

Treatment includes resection of the teratoma, if present, and initiation of immunotherapy.

There is no unanimous agreement, but immunotherapy generally starts with high doses of steroids, intravenous immunoglobulins, or plasma exchange sequentially or simultaneously. In refractory cases, cyclophosphamide or rituximab are used⁹.

In the first patient, the resection of the teratoma was rapid. However, she did not improve. Finally, it was

decided to perform an oophorectomy 5 months after the teratoma resection, followed by plasmapheresis. The patient stabilized after plasmapheresis, to the point of being sent to her secondment unit in a Glasgow coma scale 10, but without seizures and breathing freely. Recently, is possible to use a score to predict neurological function 1 year after diagnosis in patients with NMDAR encephalitis, it is called the 5-point prediction score (each parameter = 1 point), termed the anti-NMDAR encephalitis 1-year functional status (NEOS) score: (1) ICU admission required; (2) no clinical improvement after 4 weeks of treatment; (3) no treatment within 4 weeks of symptom onset; (4) abnormal MRI; and (5) CSF white blood cell count > 20 cells/ μ L¹¹.

Histological analysis showed no neoplasia in the remaining ovary.

The decision to remove an ovary without evidence of neoplasia by imaging is not easy in the context of a young patient who does not respond to conventional treatment after a teratoma in the contralateral ovary has been removed. The rationale is generally the possibility of finding an occult teratoma. The finding was negative in this case, and the patient improved after plasmapheresis.

There is a report of a 21-year-old woman with normal pelvic MRI and transabdominal ultrasound. Perioperative transvaginal ultrasound detected a first 15 mm teratoma that was resected with preservation of the right ovary. After a severe refractory clinical course, a bilateral oophorectomy was performed 6 months later, which revealed a second (6 mm) teratoma in the left ovary. However, there was no clinical improvement, and seizures persisted 12 months after the onset of symptoms¹².

There are reports of women without imaging evidence of tumor lesions, but teratomas were detected after ovarian resection. Such is the case of a 34-year-old woman with hyperkinesia, autonomic dysfunction, hypoventilation, and status epilepticus, who received intravenous immunoglobulin, rituximab, and cyclophosphamide sequentially without improvement. Initially, ovarian ultrasound and exploratory laparoscopy with bilateral biopsy were negative. Later on, the only ultrasound finding was a minimal suspicious lesion in the right ovary. Given the persistence of symptoms, a right oophorectomy was performed 11 months after the initial presentation. The cystic lesion corresponded to a mature teratoma with partial neuronal differentiation. The patient slowly improved after surgery, and 12 months later, she had reduced cognitive functions and psychomotor status, without dyskinesias, seizures, or spasms, and was able to communicate in short sentences¹³.

Johnson et al. reported the case of a 35-year-old woman with persistent non-convulsive status epilepticus who was in a coma with pentobarbital for 5 months; she received intravenous immunoglobulin, rituximab, and cyclophosphamide sequentially, without improvement. Computed tomography scans and ultrasounds of her ovaries revealed only a hemorrhagic cyst. Finally, an oophorectomy was performed, and a small teratoma was found. She woke up after 2 weeks, with slow and progressive improvement, and at 6 months, she had mild deficiencies in naming and memory tests without functional deterioration and epilepsy¹⁴.

Other authors also report women where the imaging examination was not able to detect ovarian tumors as such, but relatively small cysts interpreted as physiological, which later turned out to be teratomas that were resected, with the patients improving^{15,16}.

In the pediatric population, cases have been described in which no neoplasia was detected during the treatment of encephalitis, and the patients responded to treatment. However, during follow-up, the teratoma appeared months later, and a unilateral oophorectomy was performed. Does this mean that the neoplasia was already present? Probably, but it was not big enough to be detected by image. These patients did not have relapses of the encephalitic condition¹⁷.

Other reports have shown that patients with ovarian tumors had neither imaging nor histopathological support and yet improved after the procedure. Is this due to a microscopic teratoma that escaped histological detection or the natural history of the disease?^{18,19} One thing is clear: the search for a neoplasm is mandatory. If there is obvious evidence of a neoplasm, an oophorectomy of the involved ovary is performed, and immunotherapy is initiated.

One study compared “conservative” surgical approaches (unilateral complete or partial oophorectomy or bilateral partial oophorectomies) against “aggressive” ovarian resections (complete bilateral oophorectomy or “blind” ovarian resections without pre-operative evidence of teratoma). The study compared 23 patients: eight with aggressive resection and 15 with conservative resection. This small study concluded that aggressive approaches to ovarian resection did not confer better functional outcomes at 1 year compared with more conservative approaches in patients with NMDAR²⁰.

Conclusion

In case of suspicion of anti-NMDAR encephalitis, ovarian neoplasia should be investigated using the most

sensitive imaging methods and biomarkers available. If evidence of a tumor is found, once the patient is stabilized, the resection should be as rapid as possible to achieve the best results if there are no apparent tumor lesions, perhaps an early laparoscopic partial resection of cystic lesions, whether hemorrhagic or not, could be performed, and if there are no cystic lesions, a bilateral biopsy with histopathological study. If the neoplasia is confirmed, unilateral oophorectomy ensures reasonable lesion control. Until there are more sensitive means of identifying these neoplasms, rapid and conservative intervention combined with adequate immunological therapy and supportive measures seem most appropriate for these patients.

Acknowledgments

Our deep gratitude to Noemí Gelista-Herrera, Israel Torres-Ramírez de Arellano, and Brenda Peralta-Rodríguez for their wonderful support in histology and immunohistochemistry.

Authors' contributions

A.L. Calderón-Garcidueñas contributed to the conceptualization, formal analysis, writing the first draft, and its final revision. D.I. Talavera-Bazán contributed to the research, data extraction, and revision of the article.

Funding

This research has not received any specific grant from public, commercial, or for-profit agencies.

Conflicts of interest

The authors declare no conflicts of interest.

Ethical considerations

Protection of humans and animals. The authors declare that no experiments involving humans or animals were conducted for this research.

Confidentiality, informed consent, and ethical approval. The authors have followed their institution's confidentiality protocols, obtained informed consent from patients, and received approval from the Ethics Committee. The SAGER guidelines were followed according to the nature of the study.

Declaration on the use of artificial intelligence. The authors declare that no generative artificial intelligence was used in the writing of this manuscript.

References

- Vitaliani R, Mason W, Ances B, Zwerdling T, Jian Z, Dalmau J. Paraneoplastic encephalitis, psychiatric symptoms, and hypoventilation in ovarian teratoma. *Ann Neurol*. 2005;58:594-604.
- Dalmau J, Tüzün E, Wu HY, Masjuan J, Rossi JE, Voloschin A, et al. Paraneoplastic anti-N-methyl-D-aspartate receptor encephalitis associated with ovarian teratoma. *Ann Neurol*. 2007;61:25-36.
- Dalmau J, Armangué T, Planagumà J, Radosevic M, Mannara F, Leypoldt F, et al. An update on anti-NMDA receptor encephalitis for neurologists and psychiatrists: mechanisms and models. *Lancet Neurol*. 2019;18:1045-57.
- Dong B, Yue Y, Dong H, Wang Y. N-methyl-D-aspartate receptor hypofunction as a potential contributor to the progression and manifestation of many neurological disorders. *Front Mol Neurosci*. 2023;16:1174738.
- Song X, Luo Z, Huang D, Lv J, Xiao L, Liang T, et al. Global study of anti-NMDA encephalitis: a bibliometric analysis from 2005 to 2023. *Front Neurol*. 2024;15:1387260.
- Wu CY, Wu JD, Chen CC. The association of ovarian teratoma and anti-N-methyl-D-aspartate receptor encephalitis: an updated integrative review. *Int J Mol Sci*. 2021;22:10911.
- Chen Z, Zhang Y, Wu X, Huang H, Chen W, Su Y. Characteristics and outcomes of paroxysmal sympathetic hyperactivity in anti-NMDAR encephalitis. *Front Immunol*. 2022;13:858450.
- Ni G, Lin W, Cai X, Qin J, Feng L, Zhu S, et al. Associations between seizures and MRI in patients with anti-NMDAR encephalitis. *Acta Neurol Scand*. 2020;142:460-5.
- Nguyen L, Wang C. Anti-NMDA receptor autoimmune encephalitis: diagnosis and management strategies. *Int J Gen Med*. 2023;16:7-21.
- Herken J, Prüss H. Red flags: clinical signs for identifying autoimmune encephalitis in psychiatric patients. *Front Psychiatry*. 2017;8:25.
- Balu R, McCracken L, Lancaster E, Graus F, Dalmau J, Titulaer MJ. A score that predicts 1-year functional status in patients with anti-NMDA receptor encephalitis. *Neurology*. 2019;92:e244-52.
- Cirkel C, Cirkel A, Royl G, Frydrychowicz A, Tharun L, Deichmann S, et al. On the quest for hidden ovarian teratomas in therapy-refractory anti-NMDA receptor encephalitis: a case report. *Neurol Res Pract*. 2022;4:15.
- Boeck AL, Logemann F, Krauß T, Hussein K, Bültmann E, Trebst C, et al. Ovarectomy despite Negative Imaging in Anti-NMDA receptor encephalitis: effective even late. *Case Rep Neurol Med*. 2013;2013:843192.
- Johnson N, Henry C, Fessler AJ, Dalmau J. Anti-NMDA receptor encephalitis causing prolonged nonconvulsive status epilepticus. *Neurology*. 2010;75:1480-2.
- Zhou SX, Yang YM. Anti-N-methyl-D-aspartate receptor encephalitis with occult ovarian teratoma: a case report. *Int J Clin Exp Pathol*. 2015;8:15474-8.
- Abdul-Rahman ZM, Panegyres PK, Roeck M, Hawkins D, Bharath J, Grolman P, et al. Anti-N-methyl-D-aspartate receptor encephalitis with an imaging-invisible ovarian teratoma: a case report. *J Med Case Rep*. 2016;10:296.
- Omata T, Kodama K, Watanabe Y, Iida Y, Furusawa Y, Takashima A, et al. Ovarian teratoma development after anti-NMDA receptor encephalitis treatment. *Brain Dev*. 2017;39:448-51.
- Parratt KL, Allan M, Lewis SJ, Dalmau J, Halmagyi GM, Spies JM. Acute psychiatric illness in a young woman: an unusual form of encephalitis. *Med J Aust*. 2009;191:284-6.
- Dorigo O. Anti-N-Methyl-aspartate receptor encephalitis in identical twin sisters: role for oophorectomy. *Obstet Gynecol*. 2014;123:433-5.
- Iyengar Y, Hébert J, Climans SA, Muccilli A, Lee S, Boruah AP, et al. Ovarian resection in anti-N-methyl-D-aspartate receptor encephalitis: a comparison of surgical approaches. *Front Neurol*. 2022;13:1043785.